Available online at www.sciencedirect.com
ScienceDirect
Journal of Financial Economics 86 (2007) 213–247
JOURNAL OF Financial ECONOMICS
www.elsevier.com/locate/jfec

Stochastic skew in currency options ☆

Peter Carr[a,b], Liuren Wu[c,*]

[a]Bloomberg L.P., 731 Lexington Avenue, New York, NY 10022, USA
[b]Courant Institute, New York University, 251 Mercer Street, New York, NY 10012, USA
[c]Baruch College, Zicklin School of Business, One Bernard Baruch Way, New York, NY 10010, USA

Received 28 January 2005; received in revised form 19 November 2005; accepted 14 March 2006
Available online 29 May 2007

Abstract

We analyze the behavior of over-the-counter currency option prices across moneyness, maturity, and calendar time on two of the most actively traded currency pairs over the past eight years. We find that, on any given date, the conditional risk-neutral distribution of currency returns can show strong asymmetry. This asymmetry varies greatly over time and often switches signs. We develop and estimate a class of models that captures this stochastic skew behavior. Model estimation shows that our stochastic skew models significantly outperform traditional jump-diffusion stochastic volatility models both in sample and out of sample.

JEL classifications: G12; G13; F31; C52

Keywords: Currency options; Foreign exchange dynamics; Stochastic skew; Stochastic volatility; Time-changed Lévy processes

☆We thank G. William Schwert (the editor), an anonymous referee, Nasir Afaf, Gurdip Bakshi, Simon Benninga, Emanuel Derman, Andrew Dexter, Bernard Dumas, Bruno Dupire, Stephen Figlewski, Brian Healy, Kris Jacobs, Alireza Javaheri, Dilip Madan, John Ryan, Harvey Stein, Arun Verma, and seminar participants at Baruch College, University of California at Riverside, Columbia University, Bloomberg, Citigroup, HSBC, the 2004 European Finance Association meetings, the 2005 Winter Econometric Society meetings, and the 2005 ICBM Global Derivatives conference for comments. Any remaining errors are ours.
*Corresponding author. Tel.: +1 646 312 3509; fax: +1 646 312 3451.
E-mail address: liuren_wu@baruch.cuny.edu (L. Wu).

0304-405X/$ - see front matter © 2007 Elsevier B.V. All rights reserved.
doi:10.1016/j.jfineco.2006.03.010

1. Introduction

The foreign exchange market is the largest financial market in the world. Currently, the average trading volume in foreign currencies exceeds 1.5 trillion US dollars per day. Hence, a deeper understanding of the exchange rate dynamics has important economic repercussions. Accompanying the dizzying volume in the foreign exchange market has been a thriving over-the-counter market in currency options. Market prices of these currency options reveal important information about the underlying exchange rate dynamics. The objective of this paper is to study foreign exchange rate dynamics using currency options.

We perform our analysis using over-the-counter option quotes on two of the most actively traded currency pairs over the past eight years. The two currency pairs are the US dollar prices of the Japanese yen and the British pound. The option quotes are expressed as Garman and Kohlhagen (1983) implied volatilities at fixed time to maturities and fixed moneyness in terms of the Garman–Kohlhagen delta. For each currency pair, our data set consists of 40 option series from a matrix of eight maturities and five deltas.

From the implied volatility quotes, we find several interesting patterns. First, at each maturity, the time-series average of the implied volatility is a U-shaped function of moneyness. This well-known implied volatility smile suggests that the risk-neutral conditional distribution of currency returns is fat tailed. The average implied volatility smile persists as the option maturity increases from one week to 18 months. Second, the implied volatility at a fixed moneyness and maturity level shows substantial time variation over our sample period, suggesting that currency return volatility is stochastically time varying. Third, the curvature of the implied volatility smile is relatively stable, but the slope of the smile varies greatly over time. The sign of the slope switches several times in our sample. Therefore, although the risk-neutral distribution of the currency return exhibits persistent fat-tail behavior, the risk-neutral skewness of the distribution experiences strong time variation. It can be positive or negative on any given date.

The strong variation in currency return skewness poses a new modeling challenge for option pricing theory. Existing currency option pricing models, such as the jump-diffusion stochastic volatility model of Bates (1996b), readily accommodate the average shape of the implied volatility smiles and time variation of the implied volatility level. In the Bates model, the Merton (1976) jump component captures the short-term curvature of the implied volatility smile, whereas the Heston (1993) stochastic volatility component generates smiles at longer maturities and time variation in the implied volatility level. Unfortunately, models of this vintage cannot generate strong time variation in the risk-neutral skewness of currency returns.

Starting from the jump-diffusion stochastic volatility model of Bates (1996b), it would be tempting to try to capture stochastic skewness by randomizing the mean jump size parameter or the correlation parameter between the currency return and the stochastic volatility process, or both. In the Bates model, these two parameters govern the risk-neutral skewness at short and long maturities, respectively. However, randomizing either parameter is not amenable to analytic solution techniques that greatly aid econometric estimation.

In this paper, we attack the problem from a different perspective. We apply the general framework of time-changed Lévy processes developed in Carr and Wu (2004), and we develop a subclass of models that contrast sharply with the traditional option pricing

literature. Our models separate the up jumps from the down jumps in the currency movement through two Lévy processes. The separation is consistent with the market reality that buy orders and sell orders arrive separately in time. It also allows us to apply separate time changes to each Lévy component. Intuitively, a time change can be used to regulate the number of order arrivals that occur in a given time interval. Stochastic volatility and skewness can be induced by randomizing the time clock on which each Lévy process runs. The greater the randomness in the sum of the two clocks, the greater is the degree of stochastic volatility. The stochastic variation in the relative proportion of up and down jumps generates stochastic variation in the risk-neutral skewness of currency returns. Thus, our models are capable of generating both stochastic volatility and stochastic skewness. To differentiate this model class from traditional stochastic volatility models, we christen them as stochastic skew models (SSM).

Our parsimoniously designed stochastic skew models have one more state variable than traditional stochastic volatility models, but they have about the same number of free parameters as the Bates (1996b) model. Model estimation using options on the two currency pairs shows that our models generate much better performance in terms of both root mean squared pricing errors and log likelihood values, both in sample and out of sample. The stochastic volatility component in the Bates model can capture the time variation in overall volatility, but it cannot capture the variation in the relative proportion of up and down jumps. As a result, the Bates model and other single factor stochastic volatility models fail to capture a large portion of the variation in the currency options data. In contrast, the two random clocks in our stochastic skew models generate not only stochastic volatility, but also the stochastic skew observed in currency option prices.

Linking back to the literature, we can think of the classic Garman and Kohlhagen (1983) model as the first generation of models that captures only the stochastic variation of the currency price. The Bates (1996b) model and many other single factor stochastic volatility models also recognize the stochastic behavior of the currency return variance. Our SSM class captures the stochastic behavior of yet another dimension, the conditional skewness of the currency return distribution. Furthermore, our chosen model specifications within the SSM class capture all three dimensions with parsimony and tractability.

In other related works, Bakshi and Chen (1997) consider equilibrium valuation of foreign exchange claims. Bates (1996a) investigates the distributional properties of the currency returns implied from currency futures options. Campa and Chang (1995, 1998) and Campa, Chang, and Reider (1998) study the empirical properties of the over-the-counter currency options. Johnson (2002) proposes a stochastic volatility model of exchange rates that links both the level of volatility and its instantaneous covariance with returns to pathwise properties of the currency. By allowing time variation in the covariance, the model can generate time-varying skewness, but option pricing under this model is no longer tractable. Bollen (1998) and Bollen, Gray, and Whaley (2000) propose regime-switching models for currency option pricing. Nevertheless, Bollen and Raisel (2003) find that the jump-diffusion stochastic volatility model of Bates (1996b) outperforms regime-switching in matching the observed behaviors of currency options.

The paper is organized as follows. Section 2 describes the empirical properties of over-the-counter currency options. Section 3 develops a class of models that captures the properties of currency options. Section 4 proposes a maximum likelihood method that estimates the models using the currency option quotes. Section 5 reports the estimation

results of our parsimoniously designed stochastic skew models and compares their performance with traditional stochastic volatility models. Section 6 explores the virtues of more general specifications within the stochastic skew model class. Section 7 concludes.

2. The behavior of over-the-counter currency options

Over-the-counter currency option quotes differ from exchange-listed option quotes in two major ways. First, the over-the-counter quotes are not made directly on option prices, but on the Garman–Kohlhagen implied volatilities. Second, the implied volatilities are not quoted at a fixed strike price, but at a fixed Garman–Kohlhagen delta. Given the quote on the implied volatility, the invoice price is computed according to the Garman–Kohlhagen option pricing formula, with mutually agreed-upon inputs on the underlying spot exchange rate and interest rates. As the Garman–Kohlhagen delta is agreed upon ex ante, the strike price of the option can be derived using the Garman–Kohlhagen model and the implied volatility quote.

2.1. Data description

We collect over-the-counter currency option quotes from several broker dealers and data vendors. These data sets cover different sample periods, sampling frequencies, and currency pairs. We use the common samples of these different data sets to cross validate the quality of the data. We present the stylized evidence and estimate our models using two currency pairs from one data source because the samples on these two currency pairs span the longest time period, from January 24, 1996 to January 28, 2004. Although our data are available daily, we sample the data weekly on every Wednesday to avoid weekday effects in model estimation. Each series contain 419 weekly observations.

The two currency pairs are the dollar price of Japanese yen (JPYUSD) and the dollar price of British pound (GBPUSD). Options on each pair have eight fixed time to maturities at one week and one, two, three, six, nine, 12, and 18 months. At each maturity, quotes are available at five deltas in the form of delta-neutral straddle implied volatilities, ten- and 25-delta risk reversals, and ten- and 25-delta butterfly spreads. Altogether, we have 16,760 options quotes for each currency pair.

A straddle is a portfolio of a call option and a put option with the same strike and maturity. For the straddle to be delta-neutral under the Garman–Kohlhagen model, the strike price K needs to satisfy

$$e^{-r_f\tau}N(d_1) + e^{-r_f\tau}N(-d_1) = 0, \tag{1}$$

where r_f denotes the foreign interest rate, $N(\cdot)$ denotes the cumulative normal distribution, and

$$d_1 = \frac{\ln(F_t/K)}{IV\sqrt{\tau}} + \frac{1}{2}IV\sqrt{\tau}, \tag{2}$$

with F_t being the forward currency price, τ the time to maturity in years, and IV the implied volatility quote. Eq. (1) implies that $d_1 = 0$. Hence, the strike price is very close to the spot or forward price. We refer to this quote as the at-the-money implied volatility quote (ATMV).

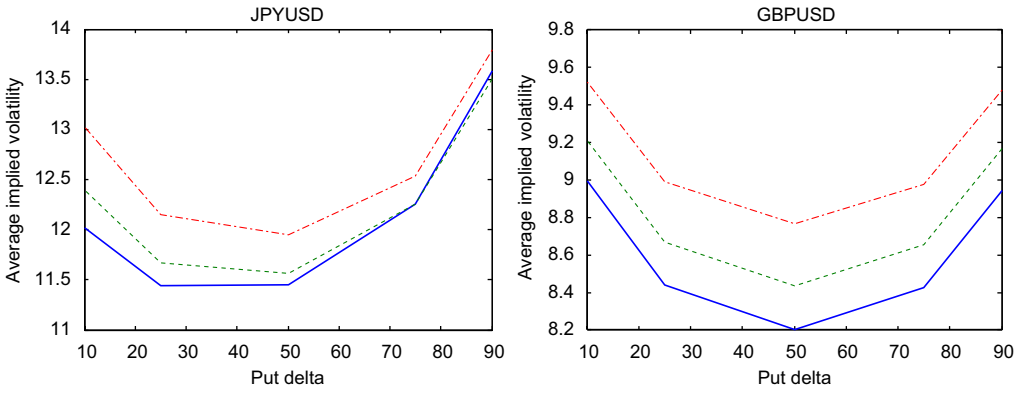

Fig. 1. Average implied volatility smiles on currency options. Lines plot the time-series average of the implied volatility quotes in percentage points against the put delta of the currency options at three selected maturities: one month (solid lines), three months (dashed lines), and 12 months (dash–dotted lines). The averages are on weekly data from January 24, 1996, to January 28, 2004, with 419 observations for each series.

The ten-delta risk reversal (RR10) quote measures the difference in implied volatilities between a ten-delta call option and a ten-delta put option,

$$RR10 = IV(10c) - IV(10p), \tag{3}$$

where $10p$ and $10c$ denote a ten-delta put and call, respectively.[1] Hence, the risk reversal is a measure of asymmetry, or slope, of the implied volatility smile across moneyness.

The ten-delta butterfly spread (BF10) measures the difference between the average implied volatility of the two ten-delta options and the delta-neutral straddle implied volatility,

$$BF10 = (IV(10c) + IV(10p))/2 - ATMV. \tag{4}$$

Hence, a butterfly spread measures the curvature of the implied volatility smile. The 25-delta risk reversals (RR25) and butterfly spreads (BF25) are defined analogously.

From the five quotes, we can derive the implied volatilities at the five levels of delta. To convert the implied volatilities into option prices and the deltas into strike prices, we need the currency price and the domestic and foreign interest rates. The currency prices are from the same data source. We strip the continuously compounded interest rates using LIBOR and swap rates from Bloomberg for the three currencies, assuming piecewise constant forward rates.

2.2. Stylized features of currency option implied volatilities

Using the currency option implied volatility quotes, we find several important features that a currency option pricing model should accommodate.

[1]As an industry convention, the deltas are quoted on out-of-money options and in absolute percentage terms. Thus, the moneyness is represented in terms of call delta when $K > F_t$ and put delta when $K < F_t$. A ten-delta call corresponds to a Garman–Kohlhagen delta of 0.1 on the call option, and a ten-delta put corresponds to a Garman–Kohlhagen delta of -0.1 on the put option.

2.2.1. The average behavior of implied volatility smiles

When we plot the time-series average of implied volatilities against delta, we observe a U shape for each currency and at each maturity. Fig. 1 plots the average implied volatility smile across moneyness at selected maturities of one month (solid lines), three months (dashed lines) and 12 months (dash–dotted lines). In the graphs, we denote the x-axis in terms of approximate put option delta. We approximate the ten-delta call as a 90-delta put in the graph and denote the delta-neutral straddle at 50 delta.

The Garman–Kohlhagen model assumes a normal currency return distribution. The smile shape of the implied volatility across moneyness has long been regarded as evidence for return non-normality under the risk-neutral measure. The curvature of the smile reflects fat tails or positive excess kurtosis in the risk-neutral return distribution. The asymmetry of the smile reflects asymmetry or skewness in the currency return distribution. The relatively symmetric mean implied volatility smiles on GBPUSD show that, on average, the risk-neutral return distribution of this currency pair is fat tailed but not highly asymmetric. In contrast, the average smiles on JPYUSD show more pronounced asymmetry.

A classic hypothesis is that return increments are independently and identically distributed (iid), with the common distribution being non-normal but with finite return variance. Under this hypothesis, the short-term return distribution is non-normal, but this non-normality disappears rapidly as the time horizon for the return increases. By virtue of the central limit theorem, the return skewness declines like the reciprocal of the square root of the time horizon, and the excess kurtosis declines like the reciprocal of the time horizon. Mapping this declining non-normality to the implied volatility smile at different maturities, we would expect the smile to flatten out rapidly at long option maturities.

Fig. 1 shows that the average smiles remain highly curved as the option maturity increases from one month to one year. This maturity pattern indicates that the risk-neutral distribution remains highly non-normal as the horizon increases. An iid return distribution with finite return variance cannot generate this average maturity pattern of the implied volatility smile. In continuous time finance, one generates iid return increments by assuming that currency returns are driven by a Lévy process. To slow down the convergence of the return distribution to normality, researchers have proposed incorporating a persistent stochastic volatility process into the return dynamics.

2.2.2. The dynamic properties of implied volatilities, risk reversals, and butterfly spreads

Fig. 2 plots the time series of the three-month delta-neutral straddle implied volatility for the two currency pairs JPYUSD and GBPUSD. The implies volatility series at other maturities show similar patterns. The plots show that, historically, the implied volatilities on both currency pairs have experienced large variations. If we use the implied volatility as a proxy for the currency return volatility level, the time-series plots in Fig. 2 suggest that a reasonable model should allow the currency return volatility to vary over time. Stochastic volatility models such as Heston (1993) and Hull and White (1987) can accommodate this feature of the data.

The market quotes on risk reversals and butterfly spreads provide direct and intuitive measures of the asymmetry and curvature of the implied volatility smile, respectively. Fig. 3 plots the time series of the three-month ten-delta risk reversals (solid lines) and butterfly spreads (dashed lines), both normalized as percentages of the corresponding delta-neutral straddle implied volatility. The ten-delta butterfly spreads are consistently at

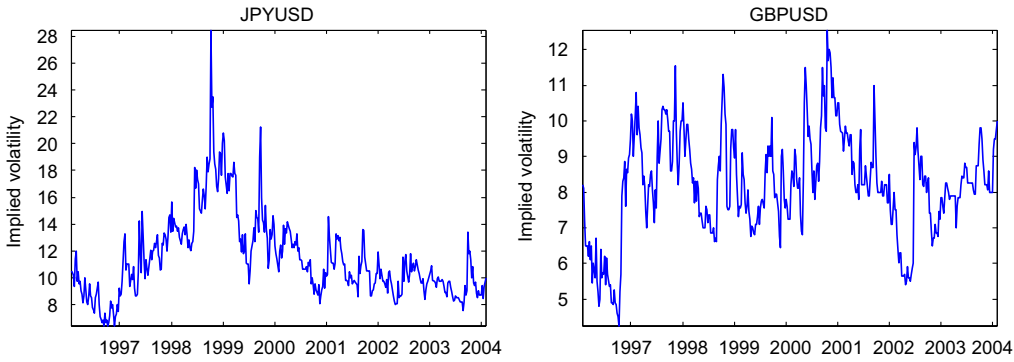

Fig. 2. The time variation of currency option implied volatilities. Lines plot the time series of the three-month delta-neutral straddle implied volatility quotes in percentage points on the dollar price of yen (JPYUSD, left panel) and pound (GBPUSD, right panel).

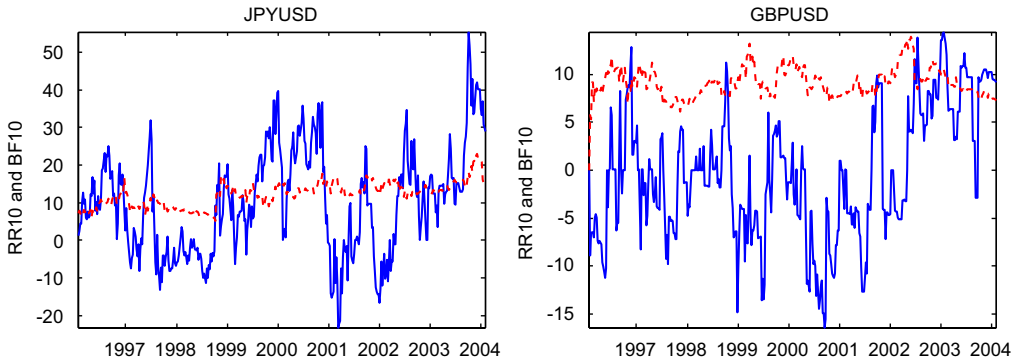

Fig. 3. Time variation of risk reversals and butterfly spreads. Solid lines are three-month ten-delta risk reversals (RR10) and dashed lines are three-month ten-delta butterfly spreads (BF10), both in percentages of the delta-neutral straddle implied volatility.

about 10% of the straddle implied volatility during the eight year span for both currency pairs. Therefore, the curvature of the smile is relatively stable over calendar time for both currency pairs. The stability suggests that excess kurtosis in the currency return distribution is a robust feature of the data.

In contrast, the risk reversals vary greatly over time. For JYPUSD, the ten-delta risk reversals have moved from −30% to 60% of the straddle implied volatility level. For GBPUSD, the swing of the ten-delta risk reversal is from −20% to 20%. For both currency pairs, the skewness of the risk-neutral return distribution varies so much that the direction of the skewness often switches. This feature of the currency options contrasts sharply with equity index options, in which the implied skewness also varies over time, but it stays highly negative across most sample periods (Foresi and Wu, 2005).

Table 1 reports the mean, standard deviation, and the weekly autocorrelation of risk reversals, butterfly spreads, and delta-neutral straddle implied volatilities. We normalize the risk reversals and butterfly spreads as percentages of the delta-neutral straddle implied volatility. For JPYUSD, the sample averages of the risk reversals are positive, implying

Table 1
Summary statistics of currency option implied volatilities

The three columns under each contract report the mean (Mean), standard deviation (Std), and weekly autocorrelation (Auto) of the contract on risk reversal (RR), butterfly spread (BF), and delta-neutral straddle implied volatilities (ATMV). Risk reversals and butterfly spreads are in percentages of the delta-neutral straddle implied volatility. The numbers following RR and BF denote the delta of the contract. Data are weekly from January 24, 1996 to January 28, 2004, with 419 observations for each series. The first column denotes the option maturities, with "w" denoting weeks and "m" denoting months.

Maturity	RR10			BF10			RR25			BF25			ATMV		
	Mean	Std	Auto	Mean	Std	Auto	Mean	Std	Auto	Mean	Std	Auto	Mean	Std	Auto
JPYUSD															
1w	15.18	16.96	0.69	14.34	4.26	0.77	7.40	8.10	0.70	4.32	1.47	0.85	11.70	3.80	0.83
1m	13.32	15.21	0.85	12.15	3.40	0.89	6.90	8.04	0.87	3.60	0.88	0.87	11.45	3.10	0.92
2m	11.53	14.27	0.89	12.08	3.21	0.92	6.02	7.63	0.91	3.51	0.67	0.87	11.47	2.84	0.94
3m	10.16	14.14	0.92	12.20	3.29	0.94	5.34	7.60	0.93	3.47	0.64	0.89	11.57	2.70	0.96
6m	8.25	14.32	0.96	12.30	3.67	0.96	4.30	7.63	0.96	3.41	0.72	0.94	11.78	2.58	0.97
9m	7.77	14.66	0.97	12.42	4.11	0.98	4.01	7.74	0.97	3.39	0.82	0.96	11.87	2.55	0.98
12m	7.45	14.99	0.97	12.39	4.48	0.98	3.81	7.91	0.97	3.34	0.90	0.97	11.95	2.53	0.98
18m	7.95	14.42	0.97	12.03	4.95	0.98	4.00	7.61	0.97	3.17	1.00	0.97	12.00	2.49	0.98
GBPUSD															
1w	−0.14	11.76	0.73	10.30	4.60	0.86	0.13	5.72	0.76	2.95	1.50	0.89	8.20	1.79	0.81
1m	−0.52	9.35	0.84	9.74	3.04	0.91	−0.11	4.68	0.84	2.95	0.86	0.88	8.20	1.47	0.90
2m	−0.33	7.48	0.88	9.22	1.83	0.87	−0.05	3.95	0.89	2.77	0.57	0.87	8.33	1.31	0.92
3m	−0.37	6.74	0.90	9.11	1.56	0.86	−0.10	3.55	0.91	2.72	0.47	0.84	8.43	1.20	0.93
6m	−0.44	5.92	0.94	8.80	1.72	0.92	0.15	3.13	0.95	2.59	0.52	0.89	8.61	1.02	0.95
9m	−0.38	5.60	0.96	8.63	1.95	0.95	−0.14	2.98	0.96	2.55	0.56	0.92	8.69	0.95	0.95
12m	−0.36	5.45	0.96	8.46	2.11	0.96	−0.14	2.91	0.97	2.49	0.55	0.92	8.77	0.90	0.95
18m	−0.53	4.93	0.97	7.99	2.38	0.97	−0.24	2.63	0.97	2.26	0.61	0.94	8.88	0.89	0.95

that the out-of-money call options are on average more expensive than the corresponding out-of-money put options during the sample period. The average butterfly spreads are around 12% at ten delta and 3∼4% at 25 delta. For GBPUSD, the average implied volatility smile is much more symmetric as the average risk reversals are close to zero. The average butterfly spreads for GBPUSD are around 9% at ten delta and less than 3% at 25 delta.

For both currencies, the standard deviations of the risk reversals are much larger than the standard deviations of the butterfly spreads. For JPYUSD, the standard deviations are around 15% for ten-delta risk reversals and are about 3∼4% for ten-delta butterfly spreads. The standard deviations of 25-delta risk reversals are about 8%, but those for the 25-delta butterfly spreads are about 1% or less. The same pattern holds for GBPUSD. The standard deviations for the risk reversals are about three times larger than those for the corresponding butterfly spreads. The delta-neutral straddle implied volatilities have standard deviations around three for JPYUSD and less than two for GBPUSD. Finally, all time series show strong serial correlation that increases with the option maturity.

2.2.3. Cross-correlations between currency returns and changes in risk reversals

Table 2 reports the cross-correlation estimates between currency returns and the weekly changes in risk reversals, butterfly spreads, and delta-neutral straddle implied volatilities.

Table 2
Cross-correlation between currency returns and weekly changes in implied volatilities

Entries report the contemporaneous correlation between log currency returns and weekly changes in risk reversals (RR), butterfly spreads (BF), and delta-neutral straddle implied volatilities (ATMV). Risk reversals and butterfly spreads are in percentages of the delta-neutral straddle implied volatility level. The numbers following RR and BF denote the delta of the contract. The first column denotes the option maturities, with "w" denoting weeks and "m" denoting months. Data are weekly from January 24, 1996 to January 28, 2004, with 419 observations for each series.

Currency	JPYUSD					GBPUSD				
maturity	RR10	BF10	RR25	BF25	ATMV	RR10	BF10	RR25	BF25	ATMV
1w	0.46	−0.06	0.48	−0.14	0.41	0.38	−0.01	0.40	−0.02	−0.02
1m	0.57	−0.06	0.58	−0.14	0.44	0.44	0.01	0.45	0.01	−0.00
2m	0.58	−0.05	0.59	−0.10	0.40	0.46	−0.01	0.46	0.02	0.02
3m	0.59	−0.06	0.59	−0.08	0.35	0.47	0.03	0.47	0.03	0.00
6m	0.59	−0.04	0.59	−0.04	0.25	0.44	0.04	0.45	0.04	0.02
9m	0.56	−0.04	0.57	−0.02	0.21	0.42	0.03	0.43	0.03	0.04
12m	0.57	−0.03	0.58	0.00	0.18	0.39	0.05	0.40	0.05	0.04
18m	0.53	−0.05	0.55	−0.01	0.18	0.37	0.06	0.37	0.07	0.02

Currency returns show strongly positive correlations with weekly changes in risk reversals across all option maturities and at both ten and 25 delta for both currency pairs. In contrast, currency returns show little correlation with changes in butterfly spreads. The correlation estimates between the currency return and changes in the delta-neutral straddle implied volatility are positive for JPYUSD, but essentially zero for GBPUSD. Hence, the only persistent and universal correlation pattern is between currency returns and risk reversals.

Using different currency pairs, sample periods, and different data sources, we have cross-validated the above-documented evidence on currency options. In particular, risk reversals on most currency pairs vary greatly over time, while butterfly spreads remain relatively stable. The positive correlations between currency returns and changes in risk reversals are also universal across most currency pairs.

3. Modeling currency return dynamics for option pricing

We propose a class of models that can capture not only the average behavior of currency option implied volatilities across moneyness and maturity, but also the dynamic variation of at-the-money implied volatilities and risk reversals.

We use $(\Omega, \mathcal{F}, (\mathcal{F}_t)_{t\geqslant 0}, \mathbb{Q})$ to denote a complete stochastic basis defined on a risk-neutral probability measure $\mathbb{Q}$, under which the log currency return obeys a time-changed Lévy process,

$$s_t \equiv \ln S_t/S_0 = (r_d - r_f)t + (L^R_{T^R_t} - \xi^R T^R_t) + (L^L_{T^L_t} - \xi^L T^L_t), \tag{5}$$

where r_d and r_f denote the continuously compounded domestic and foreign risk-free rates, respectively, both of which are assumed to be deterministic. L^R and L^L denote two Lévy processes that exhibit right (positive) and left (negative) skewness, respectively. ξ^R and ξ^L are known functions of the parameters governing these Lévy processes, chosen so that the

exponentials of $L^R_{T^R_t} - \xi^R T^R_t$ and $L^L_{T^L_t} - \xi^L T^L_t$ are both $\mathbb{Q}$ martingales. Finally, T^R_t and T^L_t denote two separate stochastic time changes applied to the two Lévy components.

In principle, the specification in Eq. (5) can capture all of the documented features of currency options. First, the two Lévy components can generate short term return non-normality and hence the implied volatility smiles at short maturities. Furthermore, by applying time changes to the two Lévy components, the model can generate stochastic volatility. Persistence in stochastic volatility reduces the speed of convergence of the return distribution to normality. Thus, the model can generate average implied volatility smiles at both short and long maturities, as well as dynamic variation in the implied volatility time series.

More important, the relative weight of the two Lévy components can also vary over time because of the separate time changes. When the weight of the right skewed Lévy component L^R is higher than the weight of the left skewed Lévy component L^L, the model generates a right skewed conditional return distribution and hence positive risk reversals. When the opposite is the case, the model generates a left skewed conditional return distribution and negative risk reversals. Thus, the model can generate variations and even sign changes on the risk reversals via the separate time changes. To stress the ability of this class of models in capturing the stochastic skewness of the currency return distribution, we christen them as stochastic skew models.

In what follows, we propose parsimonious and tractable specifications for the two Lévy components and the stochastic time changes. We then price options under the parsimoniously designed model specifications.

3.1. The Lévy components

For model design, we make the following decomposition on the two Lévy components in Eq. (5),

$$L^R_t = J^R_t + \sigma W^R_t, \quad L^L_t = J^L_t + \sigma W^L_t, \tag{6}$$

where (W^R_t, W^L_t) denote two independent, standard Brownian motions and (J^R_t, J^L_t) denote two pure jump Lévy components with positive and negative skewness in distribution, respectively.

For parsimony, we assume relative symmetry for the unconditional return distribution. We set the instantaneous volatility parameter (σ) of the two diffusion components to be the same. For the two jump components (J^R_t, J^L_t), we propose a simple yet flexible specification for the Lévy density,

$$v^R(x) = \begin{cases} \lambda e^{-\frac{|x|}{v_J}} |x|^{-\alpha-1}, & x>0 \\ 0, & x<0 \end{cases}, \quad v^L(x) = \begin{cases} 0, & x>0 \\ \lambda e^{-\frac{|x|}{v_J}} |x|^{-\alpha-1}, & x<0 \end{cases}, \tag{7}$$

so that the right skewed jump component allows only up jumps and the left skewed jump component allows only down jumps. For both jumps, we use the same parameters $(\lambda, v_J) \in \mathbb{R}^+$ and $\alpha \leqslant 2$ for parsimony. This specification has its origin in the CGMY model of Carr, Geman, Madan, and Yor (2002). We hence label it as CG jump. The Lévy density of the CG specification follows an exponentially dampened power law (Wu, 2006). Depending on the magnitude of the power coefficient α, the sample paths of the jump process can exhibit finite activity ($\alpha<0$), infinite activity with finite variation

($0 \leqslant \alpha < 1$), or infinite variation ($1 \leqslant \alpha \leqslant 2$). We need $\alpha \leqslant 2$ to maintain finite quadratic variation. Therefore, this parsimonious specification can capture a wide range of jump behaviors. We let the data determine the exact jump behavior for currency prices. Within this specification, we estimate models both with α as a free parameter and with α fixed at three special values at -1, 0, and 1. With $\alpha = -1$, the jump specification becomes a finite-activity compound Poisson process with an exponential jump size distribution as in Kou (2002). We label it as KJ jump. With $\alpha = 0$, the jump specification becomes the infinite-activity but finite variation variance-gamma model of Madan, Carr, and Chang (1998) and Madan and Seneta (1990). We hence label it as VG jump. Finally, when $\alpha = 1$, we obtain the Lévy density for an exponentially dampened Cauchy process. We label it as CJ jump.

3.2. Activity rates

We assume that the two stochastic time changes are continuous and differentiable and let

$$v_t^R \equiv \frac{\partial T_t^R}{\partial t}, \quad v_t^L \equiv \frac{\partial T_t^R}{\partial t}, \tag{8}$$

denote the instantaneous activity rates of the two Lévy components. We model the two activity rates as following square root processes,

$$\mathrm{d}v_t^j = \kappa(1 - v_t^j)\,\mathrm{d}t + \sigma_v \sqrt{v_t^j}\,\mathrm{d}Z_t^j, \quad j = R, L. \tag{9}$$

For identification, we normalize the long run mean of both processes to one. For parsimony, we set the mean reversion parameter κ and volatility of volatility coefficient σ_v to be the same for both processes.

We allow the two Brownian motions (W_t^R, W_t^L) in the return process and the two Brownian motions (Z_t^R, Z_t^L) in the activity rates to be correlated,

$$\rho^R\,\mathrm{d}t = \mathrm{E}[\mathrm{d}W_t^R\,\mathrm{d}Z_t^R], \quad \rho^L\,\mathrm{d}t = \mathrm{E}[\mathrm{d}W_t^L\,\mathrm{d}Z_t^L]. \tag{10}$$

The four Brownian motions are assumed to be independent otherwise. Furthermore, we constrain ρ^R to be positive and ρ^L to be negative. With this constraint, we generate positive skewness at short horizons via the up jump Lévy component J^R and at long horizons via the positive correlation ρ^R. Similarly, we generate negative skewness at short horizons via the down jump Lévy component J^L and at long horizons via the negative correlation ρ^L. The time variation in the relative magnitudes of the two activity rates (v_t^R and v_t^L) generates time variation in the skewness of the currency return distribution at both short and long horizons.

The correlation assumptions also capture the observed positive correlation between currency returns and changes in risk reversals. To see this, we can use $\mathrm{d}Z_t^R - \mathrm{d}Z_t^L$ to proxy the innovation in the risk reversal and $\mathrm{d}W_t^R + \mathrm{d}W_t^L$ to proxy the innovation in the currency return, ignoring the orthogonal jump component and the relative scales. Then, the correlation between currency returns and changes in risk reversals is positively related to $\rho^R - \rho^L$, which is positive given the positivity constraint on ρ^R and the negativity constraint on ρ^L.

3.3. Option pricing under stochastic skew models

For each model considered in this paper, we first derive the generalized Fourier transform of the currency return s_t and then price European options using a fast Fourier inversion method. The generalized Fourier transform of the currency return is defined as

$$\phi_s(u) \equiv \mathrm{E}[\mathrm{e}^{\mathrm{i}us_t}], \quad u \in \mathscr{D} \subset \mathbb{C}, \tag{11}$$

where $\mathrm{E}[\cdot]$ denotes the expectation operator under the risk-neutral measure $\mathbb{Q}$, and $\mathscr{D}$ is a subset of the complex domain $\mathbb{C}$ on which the expectation is well defined.

For time-changed Lévy processes, Carr and Wu (2004) show that the problem of deriving the generalized Fourier transform can be converted into an equivalent problem of deriving the Laplace transform of the random time change under a new, complex valued measure:

$$\begin{aligned}\phi_s(u) &= \mathrm{e}^{\mathrm{i}u(r_d-r_f)t}\mathrm{E}[\mathrm{e}^{\mathrm{i}u(L^R_{T^R_t}-\xi^R T^R_t)+\mathrm{i}u(L^L_{T^L_t}-\xi^L T^L_t)}] \\ &= \mathrm{e}^{\mathrm{i}u(r_d-r_f)t}\mathrm{E}^{\mathbb{M}}[e^{-\psi^\top T_t}] \equiv \mathrm{e}^{\mathrm{i}u(r_d-r_f)t}\mathscr{L}^{\mathbb{M}}_T(\psi),\end{aligned} \tag{12}$$

where $\psi \equiv [\psi^R, \psi^L]^\top$ denotes the vector of the characteristic exponents of the concavity adjusted right and left skewed Lévy components, respectively, and $\mathscr{L}^{\mathbb{M}}_T(\psi)$ represents the Laplace transform of the stochastic time vector $T_t \equiv [T^R_t, T^L_t]$ under a new measure $\mathbb{M}$. The measure $\mathbb{M}$ is defined by a complex valued exponential martingale,

$$\left.\frac{\mathrm{d}\mathbb{M}}{\mathrm{d}\mathbb{Q}}\right|_t \equiv \exp[\mathrm{i}u(L^R_{T^R_t} - \xi^R T^R_t) + \mathrm{i}u(L^L_{T^L_t} - \xi^L T^L_t) + \psi^R T^R_t + \psi^L T^L_t]. \tag{13}$$

The solution to the Laplace transform depends on the characteristic exponents and the activity rate dynamics.

The characteristic exponent of a Lévy process X is given by the Lévy–Khintchine Theorem:

$$\psi(u) \equiv \frac{1}{t}\ln\,\mathrm{E}[\mathrm{e}^{\mathrm{i}uX_t}] = -\mathrm{i}u\mu + \frac{1}{2}u^2\sigma^2 + \int_{\mathbb{R}^0}(1 - \mathrm{e}^{\mathrm{i}ux} + \mathrm{i}ux1_{|x|<1})v(x)\,\mathrm{d}x, \tag{14}$$

where μ describes the constant drift of the process, σ^2 is the constant variance rate of the diffusion component of the process, and $v(x)$ determines the arrival rate of jumps of size x and is referred to as the Lévy density (Bertoin, 1996). The truncation function $1_{|x|<1}$ equals one when $|x|<1$ and zero otherwise. It is needed under infinite variation jump processes to guarantee finiteness of the integral.

Under our Lévy density specification in Eq. (7), the integral in Eq. (14) can be carried out analytically (Wu, 2006). Table 3 summarizes the characteristic exponents of the two concavity adjusted Lévy components $(L^R_t - \xi^R t, L^L_t - \xi^L t)$ under each α specification. The characteristic exponents for the general case (CG) are applicable to all admissible α values except for two singular cases at $\alpha = 0$ and $\alpha = 1$, which have different functional forms for the characteristic exponents.

Because the Laplace transform of the time change in Eq. (12) is defined under the complex measure $\mathbb{M}$, we need to obtain the activity rate process under $\mathbb{M}$. By Girsanov's Theorem, under measure $\mathbb{M}$, the diffusion coefficient of $v(t)$ remains the same as

Table 3
Characteristic exponents of different Lévy components

All Lévy specifications have a diffusion component. The characteristic exponent for the concavity adjusted diffusion component, $\sigma W_t - \frac{1}{2}\sigma^2 t$, is $\psi^D = \frac{1}{2}\sigma^2(iu + u^2)$. Entries in the table show the characteristic exponents of the concavity adjusted Lévy jump components ($J_t^j - \xi^j t$, $j = R, L$) under different jump specifications: the finite-activity exponentially distributed jump model (KJ), the variance-gamma model (VG), the exponentially dampened Cauchy model (CJ), and the general exponentially dampened power law model (CG). The models differ in the power coefficients α, which are given in the second column of the table.

Model	α	Right skewed component ψ^R	Left skewed component ψ^L
KJ	-1	$-iu\lambda\left[\frac{1}{1-iuv_j}-\frac{1}{1-v_j}\right]+\psi^D$	$iu\lambda\left[\frac{1}{1+iuv_j}-\frac{1}{1+v_j}\right]+\psi^D$
VG	0	$\lambda\ln(1-iuv_j)-iu\lambda\ln(1-v_j)+\psi^D$	$\lambda\ln(1+iuv_j)-iu\lambda\ln(1+v_j)+\psi^D$
CJ	1	$-\lambda(1/v_j-iu)\ln(1-iuv_j)$ $+iu\lambda(1/v_j-1)\ln(1-v_j)+\psi^D$	$-\lambda(1/v_j+iu)\ln(1+iuv_j)$ $+iu\lambda(1/v_j+1)\ln(1+v_j)+\psi^D$
CG	Free	$\lambda\Gamma(-\alpha)\left[\left(\frac{1}{v_j}\right)^\alpha-\left(\frac{1}{v_j}-iu\right)^\alpha\right]$ $-iu\lambda\Gamma(-\alpha)\left[\left(\frac{1}{v_j}\right)^\alpha-\left(\frac{1}{v_j}-1\right)^\alpha\right]+\psi^D$	$\lambda\Gamma(-\alpha)\left[\left(\frac{1}{v_j}\right)^\alpha-\left(\frac{1}{v_j}+iu\right)^\alpha\right]$ $-iu\lambda\Gamma(-\alpha)\left[\left(\frac{1}{v_j}\right)^\alpha-\left(\frac{1}{v_j}+1\right)^\alpha\right]+\psi^D$

$\sigma_v\sqrt{v_t^j}$, $j = R, L$. The drift terms adjust as follows:

$$\mathtt{drift}(v_t^j)^{\mathbb{M}} = \kappa(1 - v_t^j) + iu\sigma\sigma_v\rho^j v_t^j, \quad j = R, L. \tag{15}$$

Both the drift and the variance are affine in the activity rates under measure $\mathbb{M}$. Under affine activity rates, the Laplace transform of T_t is exponential affine in the current level of the activity rates, (v_0^R, v_0^L):

$$\mathscr{L}_T^{\mathbb{M}}(\psi) = \exp(-b^R(t)v_0^R - c^R(t) - b^L(t)v_0^L - c^L(t)), \tag{16}$$

where

$$b^j(t) = \frac{2\psi^j(1 - e^{-\eta^j t})}{2\eta^j - (\eta^j - \kappa^j)(1 - e^{-\eta^j t})},$$
$$c^j(t) = \frac{\kappa}{\sigma_v^2}\left[2\ln\left(1 - \frac{\eta^j - \kappa^j}{2\eta^j}(1 - e^{-\eta^j t})\right) + (\eta^j - \kappa^j)t\right], \tag{17}$$

and

$$\eta^j = \sqrt{(\kappa^j)^2 + 2\sigma_v^2\psi^j}, \quad \kappa^j = \kappa - iu\rho^j\sigma\sigma_v, \quad j = R, L. \tag{18}$$

Thus, we obtain in closed form the generalized Fourier transforms for our stochastic skew specifications. Given the Fourier transform, we can compute the option values across all strikes numerically by applying fast Fourier inversion on the transform, as described in Carr and Wu (2004).

3.4. Option pricing under traditional jump-diffusion stochastic volatility models

The jump-diffusion stochastic volatility model of Bates (1996b) represents the state of the art in the currency option pricing literature. This model combines the Lévy

jump-diffusion specification of Merton (1976) with the stochastic volatility specification of Heston (1993). We label this model as MJDSV, where MJD denotes the Merton jump-diffusion specification and SV denotes the stochastic volatility component.

To compare the MJDSV model with our SSM specification, we cast the MJDSV model into the time–changed Lévy process framework and write the log return process under measure $\mathbb{Q}$ as

$$s_t = (r_d - r_f)t + (J_t(\lambda) - \xi t) + (\sigma W_{T_t} - \tfrac{1}{2}\sigma^2 T_t), \tag{19}$$

where $J_t(\lambda)$ denotes a compound Poisson Lévy pure jump process with mean arrival rate λ. Conditional on one jump occurring, the jump size in log returns is normally distributed with mean μ_J and variance v_J. The term W_t denotes a standard Brownian motion, and T_t denotes the stochastic clock with its activity rate given by $v_t = \partial T_t/\partial t$. The activity rate follows a square root process:

$$\mathrm{d}v_t = \kappa(1 - v_t)\,\mathrm{d}t + \sigma_v\sqrt{v_t}\,\mathrm{d}Z_t, \tag{20}$$

with $\rho\,\mathrm{d}t = \mathrm{E}[\mathrm{d}W_t\,\mathrm{d}Z_t]$. Eq. (19) makes it obvious that the MJDSV model generates stochastic volatility purely from the diffusion component, while keeping the jump arrival rate constant over time. If we set $\lambda = 0$, we obtain the pure diffusion stochastic volatility model of Heston (1993) as a special case. We also estimate this model and denote it as HSTSV.

Both MJDSV and HSTSV can generate stochastic volatility via the stochastic time change of the diffusion component, but neither can generate stochastic skew. Under HSTSV, return skewness is determined by the correlation parameter ρ between the diffusion in the currency return and the diffusion in the activity rate. With a fixed correlation parameter, the model cannot generate dramatically varying skews. Under MJDSV, the mean jump size μ_J also helps in generating return skewness at short maturities. However, because it is also a fixed parameter, the MJDSV model cannot generate large variations in the skewness, either. Thus, although both models can generate static skewness, neither model can generate the dynamics in skewness that are observed from the time series of currency option quotes.

There are some attempts in the literature that try to extend the Bates (1996b) model by making the mean jump size μ_J or the instantaneous correlation ρ stochastic. Both extensions can generate stochastic skew, but neither is amenable to analytic solution techniques that greatly aid econometric estimation.

4. Maximum likelihood estimation

To estimate the dynamic models using the time series data of implied volatilities, we cast the models into a state space form and estimate the models using the maximum likelihood method.

To capture the time-series dynamics, we need to specify the currency return and activity rate dynamics under the statistical measure $\mathbb{P}$. Because the return process under measure $\mathbb{P}$ has limited relevance for option pricing, we focus on the activity rate processes and leave the market price of return risk unspecified. We assume that the market price of risk on the activity rates is proportional to the square root of the activity rates:

$$\gamma(v_t^j) = \gamma\sqrt{v_t^j}, \quad j = L, R. \tag{21}$$

We use the same parameter γ for both activity rates. The $\mathbb{P}$-dynamics governing the activity rates become

$$dv_t^j = (\kappa - \kappa^P v_t^j)\,dt + \sigma_v\sqrt{v_t^j}\,dZ_t^j, \quad j = R, L, \tag{22}$$

with $\kappa^P = \kappa - \sigma_v\gamma$. We make analogous assumptions for the Bates (1996b) model.

In the state space form, we regard the two activity rates of the SSM model as the unobservable states $V_t \equiv [v_t^R, v_t^L]$ and specify the state propagation equation using a discrete time approximation of Eq. (22):

$$V_t = (1-\varphi)\theta^P + \varphi V_{t-1} + \sigma_v\sqrt{V_{t-1}\Delta t}\varepsilon_t, \tag{23}$$

where $\varphi = \exp(-\kappa^P\Delta t)$ denotes the autocorrelation coefficient with Δt being the length of the discrete time interval, and ε denotes an iid bivariate standard normal innovation. With weekly sampling frequency, the time interval is $\Delta t = 7/365$. For the Bates (1996b) model, the state variable $V_t \equiv v_t$ follows an analogous scalar process.

We construct the measurement equations based on the option prices, assuming additive, normally distributed measurement errors:

$$y_t = \mathrm{O}(V_t; \Theta) + e_t, \tag{24}$$

where y_t denotes the observed option prices at time t and $\mathrm{O}(V_t;\Theta)$ denotes the model implied values as a function of the parameter set Θ and the state vector V_t. The term e_t denotes the pricing errors. We convert the implied volatility quotes into out-of-money option prices and scale all option prices by their Garman–Kohlhagen vega. With this scaling, we assume that the pricing errors are iid normally distributed with zero mean and constant variance σ_r. The dimension of the measurement equation is 40, capturing the 40 options quotes on each date for each currency pair.

When both the state propagation equation and the measurement equations are linear in the state vector with normal innovations, the Kalman (1960) filter generates efficient forecasts and updates on the conditional mean and covariance of the state vector and the measurement series. In our application, the state propagation equation in Eq. (23) is linear in the state vector with normal innovation, but the measurement equation in Eq. (24) is nonlinear in the state vector. We use the unscented Kalman filter (Wan and van der Merwe, 2001) to handle the nonlinearity. The unscented Kalman filter approximates the posterior state density using a set of deterministically chosen sample points (sigma points). These sample points completely capture the true mean and covariance of the normally distributed state variables and, when propagated through the nonlinear functions in the measurement equations, capture the posterior mean and covariance of the option prices accurately to the second order for any nonlinearity. Let $\overline{y}_{t+1}$ and $\overline{A}_{t+1}$ denote the time-t ex ante forecasts of time-$(t+1)$ values of the measurement series and the covariance of the measurement series, respectively, obtained from the unscented Kalman filter. We construct the log likelihood value assuming normally distributed forecasting errors,

$$l_{t+1}(\Theta) = -\tfrac{1}{2}\log|\overline{A}_{t+1}| - \tfrac{1}{2}((y_{t+1} - \overline{y}_{t+1})^\top(\overline{A}_{t+1})^{-1}(y_{t+1} - \overline{y}_{t+1})). \tag{25}$$

The model parameters are chosen to maximize the log likelihood of the data series

$$\Theta \equiv \arg\max_{\Theta} \mathscr{L}(\Theta, \{y_t\}_{t=1}^{N}), \quad \texttt{with} \quad \mathscr{L}(\Theta, \{y_t\}_{t=1}^{N}) = \sum_{t=0}^{N-1} l_{t+1}(\Theta), \tag{26}$$

where $N = 419$ denotes the number of weeks in our sample of estimation.

For each currency pair, we estimate six models, which include the Heston (1993) model (HSTSV), the Bates (1996b) model (MJDSV), and four SSM models. The four SSM models differ in their respective jump specifications. We label them as KJSSM, VGSSM, CJSSM, and CGSSM, with KJ, VG, CJ, and CG denoting the four different jump structures, respectively.

The Bates (1996b) model has nine free parameters $\Theta_B = [\sigma_r, \sigma^2, \lambda, \mu_J, v_J, \kappa, \sigma_v, \rho, \kappa^P]$. The Heston (1993) constitutes a restricted version with $\lambda = v_J = \mu_J = 0$. Our SSM models with KJ, VG, and CJ jumps also have nine parameters, $\Theta_S = [\sigma_r, \sigma^2, \lambda, v_J, \kappa, \sigma_v, \rho^R, \rho^L, \kappa^P]$. The SSM model with CG jump specification (CGSSM) has one extra free parameter α that controls the type of the jump process. Furthermore, the four SSM models have two state variables (v_t^R, v_t^L) that generate both stochastic volatility and stochastic skewness in the currency return distribution. The Bates model and the Heston model have only one state variable v_t that controls the instantaneous variance of the diffusion component.

5. Results and discussion

In this section, we discuss the estimation results. First, we investigate which model best captures the time series and cross-sectional behavior of currency option implied volatilities. Second, we show how the estimated activity rate dynamics relate to the observed time variation in implied volatilities and risk reversals.

5.1. *In-sample model performance comparison*

We compare the in-sample model performance along two dimensions. First, we investigate how our new SSM models perform against traditional jump-diffusion stochastic volatility models. Second, within our new SSM model framework, we investigate which jump structure delivers the best performance in capturing the currency option price behavior.

Table 4 reports the parameter estimates and standard errors (in parentheses) for the six models on the two currency pairs based on the whole sample of eight years of data. In the last two rows of the table, we also report the root mean squared pricing error and the maximized log likelihood value for each model and each currency pair. The pricing errors are defined as the difference between the implied volatility quotes and the corresponding model generated values.

Our four SSM models markedly outperform the MJDSV model in terms of both the log likelihood values and the root mean squared pricing errors. For the currency pair JPYUSD, the log likelihood value for MJDSV is lower than values for the four SSM models by 2,605, 2,619, 2,637, and 2,685, respectively. The root mean squared error is 1.065 volatility points for MJDSV and is about 0.87 volatility points for the four SSM models. For GBPUSD, the log likelihood values for the four SSM models are also higher

Table 4
Full sample likelihood estimates of model parameters

Entries report the maximum likelihood estimates of the model parameters, standard errors (in parentheses), root mean squared pricing errors (rmse) in implied volatility percentage points, and the maximized log likelihood values ($\mathscr{L}$). The estimation uses eight years of weekly option data from January 24, 1996 to January 28, 2004 (419 weekly observations for each series). For each currency pair, we estimate six models: the Heston (1993) model (HSTSV), the Bates (1996b) model (MJDSV), and our stochastic skew models (SSM) with four different jump specifications: KJ, VG, CJ, and CG. The column under "Θ_B" denotes the parameter names for the Heston model and the Bates model. The column under "Θ_S" denotes the parameter names for our SSM models.

Currency		JPYUSD						GBPUSD					
Θ_B	Θ_S	HSTSV	MJDSV	KJSSM	VGSSM	CJSSM	CGSSM	HSTSV	MJDSV	KJSSM	VGSSM	CJSSM	CGSSM
σ^2	σ^2	0.020	0.006	0.006	0.005	0.004	0.003	0.010	0.008	0.003	0.003	0.002	0.002
		(0.000)	(0.000)	(0.000)	(0.000)	(0.000)	(0.001)	(0.000)	(0.000)	(0.000)	(0.000)	(0.000)	(0.000)
λ	λ	—	0.016	0.059	1.708	0.035	0.004	—	0.422	0.079	6.869	0.080	0.032
		(—)	(0.001)	(0.003)	(0.151)	(0.002)	(0.001)	(—)	(0.044)	(0.005)	(0.700)	(0.005)	(0.015)
v_j	v_j	—	0.497	0.029	0.045	0.104	0.270	—	0.003	0.012	0.017	0.031	0.039
		(—)	(0.013)	(0.001)	(0.001)	(0.004)	(0.056)	(—)	(0.000)	(0.000)	(0.001)	(0.001)	(0.004)
κ	κ	0.559	0.569	0.387	0.394	0.421	0.465	1.532	1.044	1.205	1.206	1.211	1.180
		(0.006)	(0.011)	(0.005)	(0.006)	(0.007)	(0.010)	(0.007)	(0.007)	(0.006)	(0.006)	(0.006)	(0.008)
σ_v	σ_v	1.837	1.210	1.675	1.657	1.582	1.566	2.198	1.737	1.429	1.447	1.505	1.492
		(0.023)	(0.022)	(0.027)	(0.028)	(0.027)	(0.031)	(0.026)	(0.023)	(0.039)	(0.040)	(0.017)	(0.018)
ρ	ρ^R	0.076	0.123	0.395	0.393	0.400	0.424	−0.023	−0.061	0.848	0.848	0.849	0.836
		(0.005)	(0.065)	(0.017)	(0.018)	(0.022)	(0.056)	(0.003)	(0.017)	(0.040)	(0.043)	(0.017)	(0.016)
μ_j	ρ^L	—	−0.210	−0.739	−0.758	−0.851	−1.000	—	0.002	−1.000	−0.999	−1.000	−1.000
		(—)	(0.024)	(0.034)	(0.036)	(0.040)	(0.144)	(—)	(0.001)	(0.047)	(0.050)	(0.000)	(0.004)
κ^P	κ^P	0.745	0.258	0.522	0.502	0.544	0.586	1.276	0.800	2.062	2.092	1.158	3.296
		(0.396)	(0.114)	(0.289)	(0.288)	(0.251)	(0.261)	(0.345)	(0.236)	(0.213)	(0.213)	(0.006)	(0.223)
σ_r	σ_r	1.045	1.002	0.704	0.703	0.703	0.700	0.198	0.184	0.148	0.148	0.148	0.148
		(0.003)	(0.003)	(0.002)	(0.002)	(0.002)	(0.002)	(0.000)	(0.000)	(0.000)	(0.000)	(0.000)	(0.000)
—	α	—	—	—	—	—	1.602	—	—	—	—	—	1.180
		—	—	—	—	—	(0.126)	—	—	—	—	—	(0.155)
rmse		1.099	1.065	0.865	0.865	0.866	0.865	0.464	0.442	0.387	0.387	0.387	0.388
$\mathscr{L}, \times 10^3$		−9.430	−9.021	−6.416	−6.402	−6.384	−6.336	4.356	4.960	6.501	6.502	6.497	6.521

than the value for the MJDSV model, with the difference ranging from 1,537 to 1,561. The root mean squared pricing error is 0.442 volatility points for MJDSV and is about 0.39 for the four SSM models. From MJDSV to its restricted version HSTSV, we observe a further reduction in likelihood values and a further increase in root mean squared pricing errors. The likelihood difference is 409 for JPYUSD and 604 for GBPUSD. These differences show that the jump component in MJDSV improves the model performance over the pure diffusion model of HSTSV.

Within our SSM framework, we estimate four models with different jump specifications. In contrast to the large difference in log likelihood values between the SSM models and the MJDSV model, the likelihood value differences among the four SSM models are much smaller. The parameter estimates for the four SSM models are also similar, except for the jump parameters, which can have different scales under different jump specifications. For JPYUSD, we detect a marginal increase in the likelihood value as we move from KJ to VG and then to the CJ jump structure. These three jump specifications differ by a power term in the Lévy density. The performance ranking corresponds to an increase in the power coefficient α and an increase in jump frequency. When we estimate the CGSSM model where α is a free parameter, the estimate for α is 1.602, indicating that a high frequency jump specification is favored for modeling JPYUSD options. Nevertheless, when we compare the root mean squared pricing errors for the four SSM models, we can hardly distinguish any differences among the four jump types. For GBPUSD, the estimate of α under the CGSSM model is 1.18, but the performance differences of the four SSM models are negligible in terms of both the log likelihood values and the root mean squared pricing errors. Therefore, we conclude that our currency options data cannot effectively distinguish between different jump types. There is only weak evidence that favors a high frequency jump specification with infinite variation for JPYUSD.

Our results on the nature of the jump specification for currency options are not as strong as those in Carr and Wu (2003) and Huang and Wu (2004) for equity index options. Both studies find that infinite activity jump specifications significantly outperform finite activity jump specifications for pricing Standard & Poor's 500 index options. Daal and Madan (2005) also find evidence that the infinite activity VG model performs better than the finite activity Merton (1976) jump in pricing currency options. Those studies use exchange-traded options that include deep out-of-money contracts. The over-the-counter currency options data that we use have only five strikes for each maturity, all located within approximately the tenth and 90th percentile of the risk-neutral return distribution. Hence, the currency options data that we use do not provide much information on the tail (beyond the tenth percentile) of the risk-neutral currency return distribution. However, it is in the tails of the distribution that the alternative jump specifications display their differences.

To test the statistical significance of the performance difference between different models, we adopt the likelihood ratio statistic constructed by Vuong (1989) for non-nested models. Formally, we let $LR(\Theta_i, \Theta_j)$ denote the log likelihood ratio between models i and j,

$$LR(\Theta_i, \Theta_j) \equiv \mathscr{L}_i(\Theta_i) - \mathscr{L}_j(\Theta_j). \tag{27}$$

Vuong constructs a test statistic based on this log likelihood ratio,

$$\mathscr{M} = LR(\Theta_i, \Theta_j)/(\hat{s}\sqrt{N}), \tag{28}$$

where N denotes the number of weeks in the time series and $\hat{s}^2$ denote the variance estimate of the weekly log likelihood ratio $(l_i - l_j)$. Vuong proves that $\mathscr{M}$ has an asymptotic

Table 5
Full sample likelihood ratio tests of model performance differences

Entries report the pairwise likelihood ratio test statistics $\mathscr{M}$ on non-nested models. The statistic has an asymptotic standard normal distribution. We report the pairwise statistics in a (6×6) matrix, with the (i,j)th element denoting the statistic on model i versus model j such that a strongly positive estimate for this element indicates that model i significantly outperforms model j. The tests are based on the model estimations using the full sample of eight years of data for each currency. We bold the lower triangular elements that are greater than 1.65, the critical value at 95% confidence level. The upper triangular elements contain the same information as the lower triangular elements, only with opposite signs.

$\mathscr{M}$	HSTSV	MJDSV	KJSSM	VGSSM	CJSSM	CGSSM
JPYUSD						
HSTSV	0.00	−2.55	−4.92	−4.88	−4.75	−4.67
MJDSV	**2.55**	0.00	−5.39	−5.33	−5.22	−5.07
KJSSM	**4.92**	**5.39**	0.00	−1.11	−0.86	−1.20
VGSSM	**4.88**	**5.33**	1.11	0.00	−0.72	−1.21
CJSSM	**4.75**	**5.22**	0.86	0.72	0.00	−1.59
CGSSM	**4.67**	**5.07**	1.20	1.21	1.59	0.00
GBPUSD						
HSTSV	0.00	−2.64	−4.70	−4.68	−4.63	−4.71
MJDSV	**2.64**	0.00	−3.85	−3.86	−3.89	−4.19
KJSSM	**4.70**	**3.85**	0.00	−0.04	0.34	−0.37
VGSSM	**4.68**	**3.86**	0.04	0.00	0.56	−0.39
CJSSM	**4.63**	**3.89**	−0.34	−0.56	0.00	−0.51
CGSSM	**4.71**	**4.19**	0.37	0.39	0.51	0.00

standard normal distribution under the null hypothesis that the two models are equivalent in terms of likelihood. Based on the weekly log likelihood estimates, we compute the sample mean and standard deviation of the likelihood ratio between each pair of models and then construct the test statistic in Eq. (28). In estimating $\widehat{s}$, we adjust for serial dependence in the weekly log likelihood ratios according to Newey and West (1987) with the lags optimally chosen following Andrews (1991) under an AR(1) specification.

Table 5 reports the pairwise log likelihood ratio test statistics. For each currency pair, we report the statistics in a (6×6) matrix, with the (i,j)th element being the statistic on $(l_i - l_j)$. Given the symmetry of the test, the diagonal terms are zero by definition and the lower triangular elements are equal to the negative of the upper triangular elements. We focus on the lower triangular entries for our discussion and use boldface type to highlight the statistics that are greater than 1.65, which corresponds to a 95% confidence level on a one-sided test.

For both currency pairs, all of the off-diagonal elements in the first column are positive and strongly significant, indicating that HSTSV is the worst performing of all six estimated models. The last four elements in the second column are also strongly positive and significant, indicating that the performance of MJDSV is significantly worse than the four SSM models. However, as we move to the (4×4) block in the right bottom corner, none of the elements is significant for either currency pair. This block compares the performance among the four SSM models, with CGSSM having an extra free parameter α that controls the jump type. Within the SSM modeling framework, our currency options data cannot effectively distinguish the different jump specifications.

5.2. Out-of-sample performance comparison

To study the out-of-sample performance, we reestimate the six models using the first six years of data from January 24, 1996 to December 26, 2001, with 310 weekly observations for each series. Then, we use these estimated model parameters to compare the model performance both in sample during the first six years and out of sample during the last two years from January 2, 2002 to January 28, 2004, with 109 weekly observations for each series. If the behavior of currency option prices has not dramatically changed during the last two years, we would expect that the out-of-sample performance for each model is similar to its in-sample performance. We also investigate whether the superior in-sample performance of our SSM models over traditional specifications such as HSTSV and MJDSV extends to an out-of-sample comparison.

Table 6 reports the subsample estimates and standard errors of the model parameters. For GBPUSD, the parameter estimates from the subsample are close to those obtained from the full sample estimation in Table 4. The differences in the two sets of estimates for most parameters are within two times their respective standard errors. The stability of parameter estimates suggest that the option price behavior on GBPUSD has not experienced dramatic structural changes over the past two years. For JPYUSD, the subsample estimates on some of parameters show substantial differences from the full sample estimates. In particular, for all six models, the subsample estimates on the mean reversion parameter κ are markedly larger than the corresponding full sample estimates. The subsample estimates for the volatility of volatility coefficients σ_v are also larger than the corresponding full sample estimates for five of the six models. These differences suggest that option price behavior on JPYUSD is not as stable as that on GBPUSD.

Table 7 compares the in-sample and out-of-sample performance of the six models based on the subsample estimation. We report the root mean squared pricing error, the mean weekly log likelihood value ($\mathscr{L}/N$), and the pairwise likelihood ratio test statistics defined in Eq. (28). To facilitate comparison between in- and out-of-sample performance, we normalize the aggregate likelihood value ($\mathscr{L}$) by the number of weeks (N) for each sample period and report the mean weekly log likelihood estimate ($\mathscr{L}/N$). The in-sample comparison is based on the first 310 weeks of data. The out-of-sample comparison is based on the last 109 weeks of data.

For each currency pair and each model, we first compare the in-sample and out-of-sample performance in terms of the root mean squared pricing error and the mean weekly log likelihood value. The in-sample and out-of-sample estimates are very close to one another. For JPYUSD, most models generate slightly larger out-of-sample pricing errors and smaller out-of-sample likelihood values than their in-sample counterpart. For GBPUSD, all models generate smaller out-of-sample pricing errors and larger out-of-sample likelihood values. Therefore, we do not observe much degeneration in out-of-sample performance.

To test the overall stability of the model parameters over time, we construct a likelihood ratio statistic. We can think of the full-sample estimates in Table 4 as for a restricted model in which the parameters during the first six years are restricted to be the same as the parameters during the last two years. By comparison, the subsample estimates in Table 6 can be regarded as for an unrestricted model as they can be different from the parameter values during the last two years. Thus, we can construct the likelihood ratio statistic based

Table 6
Subsample likelihood estimates of model parameters

Entries report the maximum likelihood estimates of the model parameters and their standard errors (in parentheses). The estimation uses the first six years of weekly option data from January 24, 1996 to December 26, 2001 (310 weekly observations for each series). For each currency pair, we estimate six models: the Heston (1993) model (HSTSV), the Bates (1996b) model (MJDSV), and our stochastic skew models (SSM) with four different jump specifications: KJ, VG, CJ, and CG. The column under "Θ_B" denotes the parameter names for the Heston model and the Bates model. The column under "Θ_S" denotes the parameter names for our SSM models.

Currency		JPYUSD						GBPUSD					
Θ_B	Θ_S	HSTSV	MJDSV	KJSSM	VGSSM	CJSSM	CGSSM	HSTSV	MJDSV	KJSSM	VGSSM	CJSSM	CGSSM
σ^2	σ^2	0.022	0.011	0.006	0.006	0.005	0.002	0.010	0.009	0.003	0.003	0.002	0.003
		(0.000)	(0.000)	(0.000)	(0.000)	(0.000)	(0.002)	(0.000)	(0.000)	(0.000)	(0.000)	(0.000)	(0.000)
λ	λ	—	0.016	0.074	2.486	0.053	0.004	—	2.027	0.087	7.829	0.091	1210
		(—)	(0.001)	(0.004)	(0.234)	(0.004)	(0.002)	(—)	(0.153)	(0.006)	(0.922)	(0.007)	(9439)
v_j	v_j	—	0.491	0.027	0.041	0.087	0.273	—	0.001	0.012	0.017	0.030	0.011
		(—)	(0.018)	(0.001)	(0.001)	(0.004)	(0.089)	(—)	(0.000)	(0.000)	(0.001)	(0.001)	(0.006)
κ	κ	0.810	0.846	0.660	0.665	0.686	0.739	1.449	1.015	1.177	1.178	1.183	1.173
		(0.006)	(0.013)	(0.006)	(0.007)	(0.008)	(0.012)	(0.008)	(0.008)	(0.007)	(0.008)	(0.008)	(0.012)
σ_v	σ_v	1.943	1.171	1.945	1.922	1.881	1.777	2.091	2.041	1.428	1.452	1.523	1.518
		(0.025)	(0.024)	(0.031)	(0.031)	(0.032)	(0.037)	(0.030)	(0.028)	(0.047)	(0.048)	(0.023)	(0.053)
ρ	ρ^R	0.050	0.062	0.270	0.267	0.252	0.299	−0.056	−0.065	0.796	0.794	0.789	0.720
		(0.005)	(0.078)	(0.015)	(0.016)	(0.018)	(0.092)	(0.005)	(0.013)	(0.047)	(0.050)	(0.022)	(0.053)
μ_j	ρ^L	—	−0.212	−0.629	−0.642	−0.672	−1.000	—	−0.001	−1.000	−0.999	−1.000	−0.905
		(—)	(0.033)	(0.035)	(0.037)	(0.041)	(0.396)	(—)	(0.000)	(0.059)	(0.062)	(0.000)	(0.069)
κ^P	κ^P	1.090	0.636	0.924	0.879	0.822	0.813	1.308	2.529	2.022	2.060	1.166	2.192
		(0.390)	(0.155)	(0.392)	(0.385)	(0.364)	(0.331)	(0.451)	(0.238)	(0.263)	(0.260)	(0.270)	(0.263)
σ_r	σ_r	1.095	1.072	0.746	0.747	0.746	0.744	0.217	0.200	0.175	0.175	0.175	0.174
		(0.003)	(0.004)	(0.002)	(0.002)	(0.002)	(0.002)	(0.001)	(0.001)	(0.001)	(0.001)	(0.001)	(0.001)
—	α	—	—	—	—	—	1.691	—	—	—	—	—	−1.162
		—	—	—	—	—	(0.175)	—	—	—	—	—	(15.37)

Table 7
In-sample and out-of-sample model performance comparison

Entries report the root mean squared pricing error (rmse) in implied volatility percentage points, mean weekly log likelihood value ($\mathscr{L}/N$), and the pairwise likelihood ratio test statistics $\mathscr{M}$ on non-nested models. The models are estimated using data from January 24, 1996 to December 26, 2001 (310 weekly observations for each series). The in-sample statistics are from the same period. The out-of-sample statistics are computed from the remaining two years of data from January 2, 2002 to January 28, 2004 (109 weekly observations for each series) based on model parameter estimated from the first subsample. The last panel reports the likelihood ratio test statistics $LR = 2(\mathscr{L}_{\text{Sub}} - \mathscr{L}_{\text{Full}})$ and their corresponding 99% critical values (CV) between the models estimated using the first six years of data and the corresponding models estimated using the full sample of eight years of data. The likelihood ratio is computed based on the first six years of data.

Currency	JPYUSD						GBPUSD					
Model	HSTSV	MJDSV	KJSSM	VGSSM	CJSSM	CGSSM	HSTSV	MJDSV	KJSSM	VGSSM	CJSSM	CGSSM
In-sample performance												
rmse	1.14	1.11	0.89	0.89	0.89	0.89	0.49	0.46	0.42	0.42	0.42	0.42
$\mathscr{L}/N$	−23.69	−23.03	−16.61	−16.60	−16.57	−16.47	8.36	10.06	12.27	12.27	12.26	12.28
$\mathscr{M}$												
HSTSV	0.00	−2.14	−4.44	−4.41	−4.33	−4.17	0.00	−3.34	−4.42	−4.39	−4.24	−4.33
MJDSV	**2.14**	0.00	−4.74	−4.70	−4.61	−4.42	**3.34**	0.00	−3.40	−3.39	−3.33	−3.33
KJSSM	**4.44**	**4.74**	0.00	−0.49	−0.51	−0.84	**4.42**	**3.40**	0.00	0.08	0.36	−0.42
VGSSM	**4.41**	**4.70**	0.49	0.00	−0.51	−0.89	**4.39**	**3.39**	−0.08	0.00	0.51	−0.42
CJSSM	**4.33**	**4.61**	0.51	0.51	0.00	−1.14	**4.24**	**3.33**	−0.36	−0.51	0.00	−0.55
CGSSM	**4.17**	**4.42**	0.84	0.89	1.14	0.00	**4.33**	**3.33**	0.42	0.42	0.55	0.00
Out-of-sample performance												
rmse	1.09	1.03	0.90	0.90	0.90	0.90	0.40	0.38	0.27	0.27	0.27	0.27
$\mathscr{L}/N$	−24.01	−21.75	−18.47	−18.35	−18.23	−18.11	14.36	15.85	23.30	23.29	23.26	23.25
$\mathscr{M}$												
HSTSV	0.00	−6.01	−5.90	−6.01	−6.08	−6.12	0.00	−4.88	−7.06	−7.06	−7.05	−7.05
MJDSV	**6.01**	0.00	−3.11	−3.23	−3.32	−3.48	**4.88**	0.00	−5.98	−5.99	−5.99	−5.97
KJSSM	**5.90**	**3.11**	0.00	−7.76	−6.81	−5.27	**7.06**	**5.98**	0.00	0.64	1.47	4.51
VGSSM	**6.01**	**3.23**	**7.76**	0.00	−4.39	−3.67	**7.06**	**5.99**	−0.64	0.00	1.63	4.19
CJSSM	**6.08**	**3.32**	**6.81**	**4.39**	0.00	−3.11	**7.05**	**5.99**	−1.47	−1.63	0.00	0.23
CGSSM	**6.12**	**3.48**	**5.27**	**3.67**	**3.11**	0.00	**7.05**	**5.97**	**−4.51**	**−4.19**	−0.23	0.00
Likelihood ratio tests for overall parameter stability over time												
LR	663.8	600.8	857.6	854.6	863.0	859.8	357.4	498.8	263.4	264.0	265.6	318.4
CV	16.8	21.7	21.7	21.7	21.7	23.2	16.8	21.7	21.7	21.7	21.7	23.2

on the first six years of data, $LR = 2(\mathscr{L}_{\text{Sub}} - \mathscr{L}_{\text{Full}})$, where the subscript *Sub* and *Full* refer, respectively, to the subsample and full sample parameter estimates used to compute the likelihoods for the six years of data. The statistic has a chi-square distribution with six degrees of freedom for HSTSV; nine degrees of freedom for MJDSV, KJSSM, VGSSM, and CJSSM; and ten degrees of freedom for CGSSM. We report the likelihood ratio statistic, as well as the critical values at 99% confidence level in the last panel of Table 7. The statistics suggest that the null hypothesis that the parameters are the same during the two sample periods are rejected.

We now compare the performance of different models both in sample and out of sample. The root mean squared error and the log likelihood values in Table 7 show that the four SSM models perform much better than the MJDSV and HSTSV models, both in sample and out of sample. The likelihood ratio test statistics $\mathscr{M}$ tell the same story. For both in-sample and out-of-sample tests, the off-diagonal terms in the first column of the $\mathscr{M}$ matrix are all strongly positive for both currencies, indicating that all other models significantly outperform the Heston (1993) model. The last four elements of the second column are also strongly positive, indicating that our four SSM models significantly outperform the MJDSV model.

Among the four SSM models, the in-sample $\mathscr{M}$ statistics show that the four models are not statistically different from one another for both currencies. For out-of-sample performance on JPYUSD, the CG jump structure significantly outperforms the three restricted jump specifications (KJ, VG, and CJ). Among the three restricted jump specifications, CJ significantly outperforms KJ and VG, and VG significantly outperforms KJ, thus generating the following statistically significant performance ranking in descending order: CG, CJ, VG, and KJ. The qualitative conclusion is similar to that from the in-sample comparison, but statistically stronger: High frequency jumps perform better in capturing the option price behavior on JPYUSD.

For GBPUSD, the out-of-sample performance ranking among the four jump specifications goes the opposite direction, but with less statistical significance. Although the encompassing CG jump specification generates slightly better in-sample performance, its out-of-sample performance is significantly worse than KJ and VG. Thus, options on GBPUSD ask for a more parsimonious and less frequent jump specification.

Historically, JPYUSD options have generated much larger smile curvature (butterfly spreads) and skews (risk reversals) than options on GBPUSD. Thus, we conclude that high frequency jump specifications perform better in capturing large return non-normality, but a finite activity jump specification suffices for capturing moderate non-normality in the return distribution.

In summary, likelihood ratio tests reject the null hypothesis on all models that the model parameters do not vary over the eight years of sample period. Nevertheless, our estimated SSM models significantly outperform traditional jump-diffusion stochastic volatility models regardless of the sample period and irrespective of whether the test is in sample or out of sample.

5.3. Pricing biases

Another way to investigate the performance of different models is to check for the existence of any structural patterns in the pricing errors of these models. Because we have documented the evidence mainly in the implied volatility space, we also define the pricing

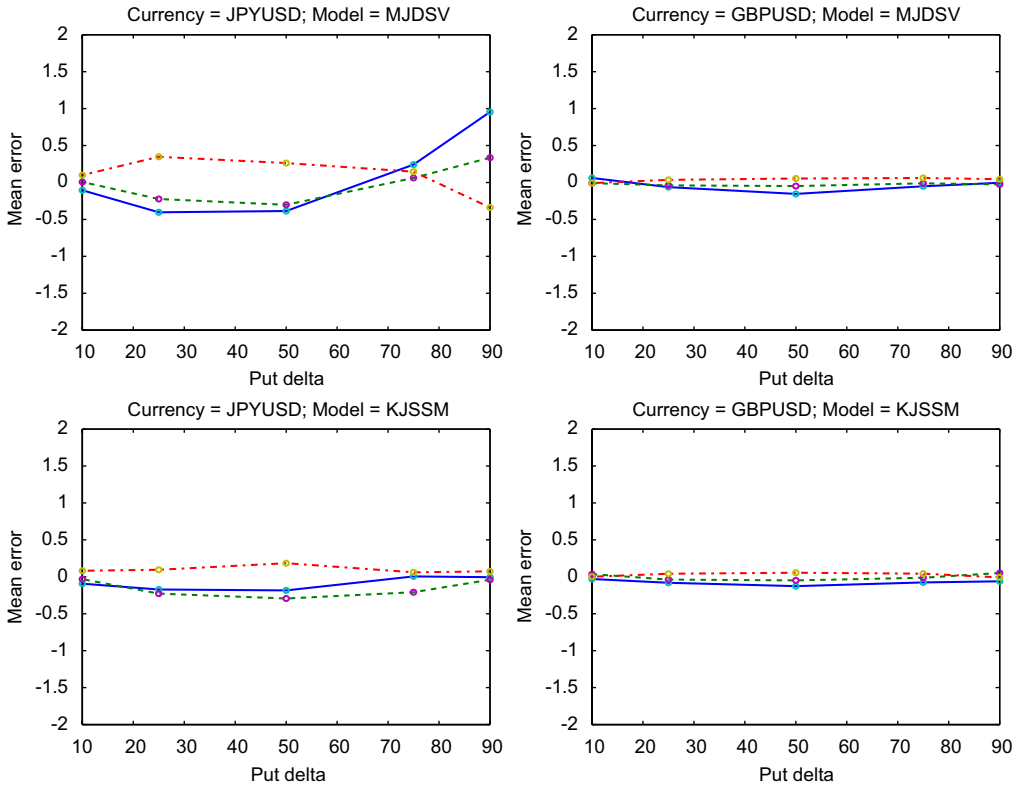

Fig. 4. Mean pricing error. The three lines in each panel denote the mean pricing errors across moneyness at three maturities: one month (solid lines), three months (dashed lines), and 12 months (dash–dotted lines). The pricing errors are defined as the difference between the observed implied volatility quote in percentage points and the corresponding model values.

errors in the volatility space as the difference between the observed implied volatility quote and the corresponding values computed from the model.

The mean pricing error of a good model should be close to zero and show no obvious structures along both the moneyness and the maturity dimensions. Fig. 4 plots the mean pricing error in volatility percentage points along the moneyness dimension at selected maturities of one month (solid lines), three months (dashed lines), and 12 months (dash–dotted lines). Because the in-sample and out-of-sample performances are similar for all models, we report results only from the full sample estimation. To further reduce graphics clustering, we henceforth focus on two models, one from our four SSM specifications and one from the two traditional specifications. The four SSM models generate similar performance. We choose KJSSM as the representative. Of the two traditional models, the Bates model (MJDSV) performs better than the pure diffusion Heston model (HSTSV). We choose the better performing MJDSV and compare its performance with KJSSM.

Under the MJDSV model, the mean pricing errors display obvious structural patterns for JPYUSD along both the moneyness and maturity dimensions. At short maturities, the mean pricing errors show a smile shape along the moneyness dimension, implying that the

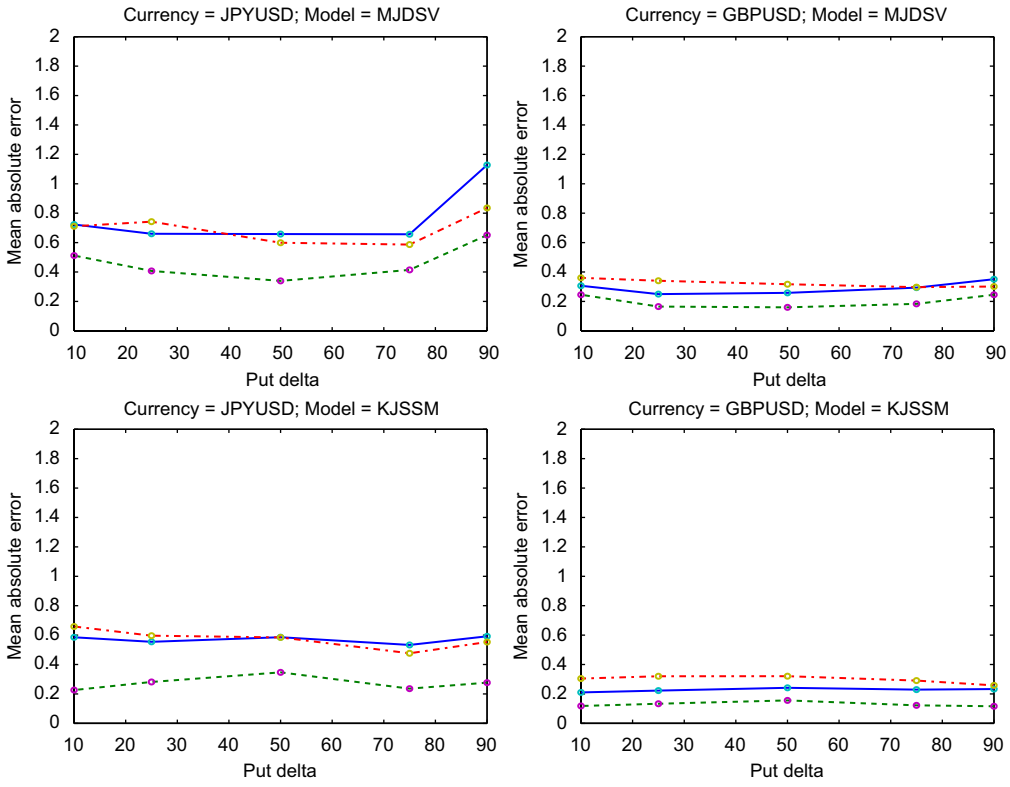

Fig. 5. Mean absolute pricing error. The three lines in each panel denote the mean absolute pricing errors across moneyness at three maturities: one month (solid lines), three months (dashed lines), and 12 months (dash–dotted lines). The pricing errors are defined as the difference between the observed implied volatility quote in percentage points and the corresponding model values.

MJDSV model cannot fully account for the implied volatility smile at short maturities. At longer maturities, the mean pricing errors show an inverse smile shape along the moneyness dimension, implying that the MJDSV model generates excess curvature in the implied volatility smile at these maturities. In contrast, under our KJSSM model, the mean pricing errors are very close to zero and do not show any obvious remaining structural patterns. For both currencies, the mean pricing errors under KJSSM are all well within half a percentage point, the average bid-ask spread for the implied volatility quotes.

Fig. 5 plots the mean absolute pricing error in implied volatility under MJDSV and KJSSM. Under both models, the mean absolute pricing errors are smaller for GBPUSD than for JPYUSD. Under MJDSV, the mean absolute pricing errors are larger on out-of-money options than on at-the-money options, indicating that the MJDSV model cannot fully account for the observed implied volatility smile. The mean absolute pricing errors are also larger at very short and long maturities than at moderate maturities, indicating that the model cannot fully account for the term structure of the implied volatilities.

The mean absolute pricing errors under KJSSM are smaller than those under MJDSV across all moneyness levels and maturities for both currency pairs. Hence, this SSM model performs universally better than the MJDSV model. Furthermore, under KJSSM, the

mean absolute pricing error is invariant to moneyness at each maturity and for each underlying currency pair, indicating that the model captures the volatility smile at all terms and for both currencies. Along the maturity dimension, the mean absolute pricing errors are smaller at moderate maturities than at very short and very long maturities, indicating that the model has some remaining tensions along the term structure dimension.

5.4. The activity rate dynamics

Under the SSM models, the risk-neutral dynamics of the two activity rates are mainly controlled by two parameters: κ and σ_v. The parameter κ controls the speed of mean reversion for the activity rate processes. The parameter σ_v controls the instantaneous volatility of the processes. Furthermore, the activity rate processes interact with the currency return innovation through the instantaneous correlation parameters ρ^R and ρ^L. Under the statistical measure, the time-series dynamics of the activity rates differ from the risk-neutral dynamics in terms of the mean reverting speeds κ^P. The difference between κ and κ^P captures the market price of volatility risk. When the market price of risk coefficient γ is positive, the time-series dynamics of the activity rates are more persistent. The opposite is true when the coefficient is negative.

In Table 4, the estimates for the risk-neutral mean reversion speed κ in the SSM models for JPYUSD vary from 0.387 to 0.465 as the jump specification changes. The statistical mean reversion speeds κ^P are slightly larger, ranging from 0.502 to 0.586. The difference between the two sets of parameters imply that the market price of activity rate risk is negative. For GBPUSD, the κ estimates are larger between 1.18 and 1.211. The corresponding time-series estimates are between 1.158 and 3.296, implying a negative market price of risk except under CJSSM. Intuitively, the activity rate captures the volatility of the exchange rate. A negative market price for the activity rate risk implies that investors are averse to both high activity level and high variation in the activity rate. Nevertheless, our inference on the signs of market prices of risk is tentative, given the large standard errors on the estimates for κ^P.

The estimates for the instantaneous volatility coefficient of the activity rates σ_v are also stable across different jump specifications under the SSM framework. The estimates are between 1.566 and 1.675 for JPYUSD and between 1.429 and 1.505 for GBPUSD.

The estimates for the instantaneous correlation are significantly positive between the positively skewed Lévy component and its activity rate, and they are strongly negative between the negatively skewed Lévy component and its activity rate. These different correlations help in generating the stochastic skews at long maturities. They also help generate the observed positive correlation between currency returns and changes in risk reversals.

Under the HSTSV and MJDSV models, a scalar activity rate process controls the overall stochastic volatility. The estimates for the persistence parameters κ and κ^P and the instantaneous volatility parameter σ_v are similar to those obtained under the SSM models. However, the instantaneous correlation ρ estimates are close to zero under both currencies, consistent with our observation that the currency returns and changes in volatilities do not have strong cross-correlations.

The unscented Kalman filter provides a fast way to update the activity rates to achieve an approximate fit to the implied volatility surface. In Fig. 6, the top two panels plot the filtered activity rates for the MJDSV model, and the bottom two panels plot the filtered

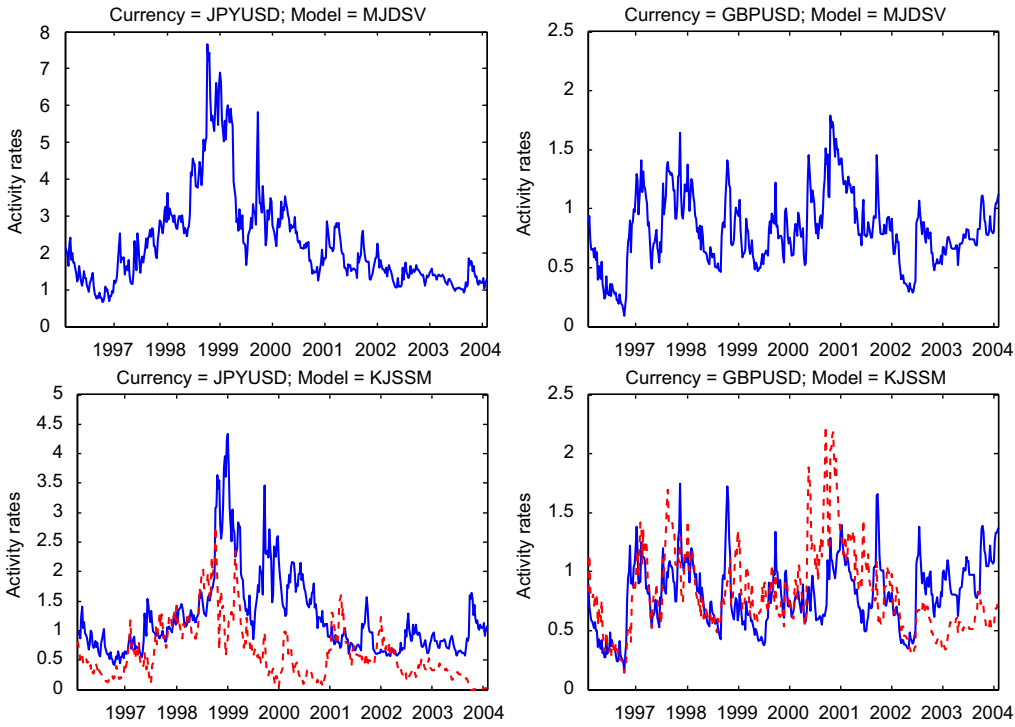

Fig. 6. Time series of the activity rates. The top two panels plot the single series of the activity rates from the MJDSV model. The bottom two panels plot the two activity rate series from the KJSSM model, where the solid lines denote the activity rate for the right skewed Lévy component and the dashed lines denote the activity rate for the left skewed Lévy component. We extract the activity rates from the options data using unscented Kalman filter, based on the estimated models using the whole sample of data.

activity rates of the right skewed (solid lines) and left skewed (dashed lines) return components under the KJSSM model.

Under both models, the overall time variation of the activity rates match the ups and downs in the time series of the implied volatilities in Fig. 2. Hence, both models can capture the stochastic volatility feature of currency options. For example, the implied volatilities on JPYUSD show a large spike between 1998 and 1999, reflecting the market stress during the Russian bond crisis and the ensuing hedge fund crisis. The single activity rate process under MJDSV shows a similar spike. The two activity rates from our SSM model tell a more detailed story. The spike in the implied volatility was mainly caused by a spike in the activity rate level for the right skewed Lévy component, whereas the activity rate level for the left skewed Lévy component went down. The difference in the two activity rates during the hedge fund crisis reveals a potential imbalance of market demand for out-of-money call and put options on the Japanese yen. The industry folklore is that many hedge funds had gone short on yen before the crisis and were then forced to use call options to cover their positions during the crisis. This extra demand for call options on yen drove up the activity rate of upward yen moves (solid line), but not the activity rate of downward yen moves (dashed line).

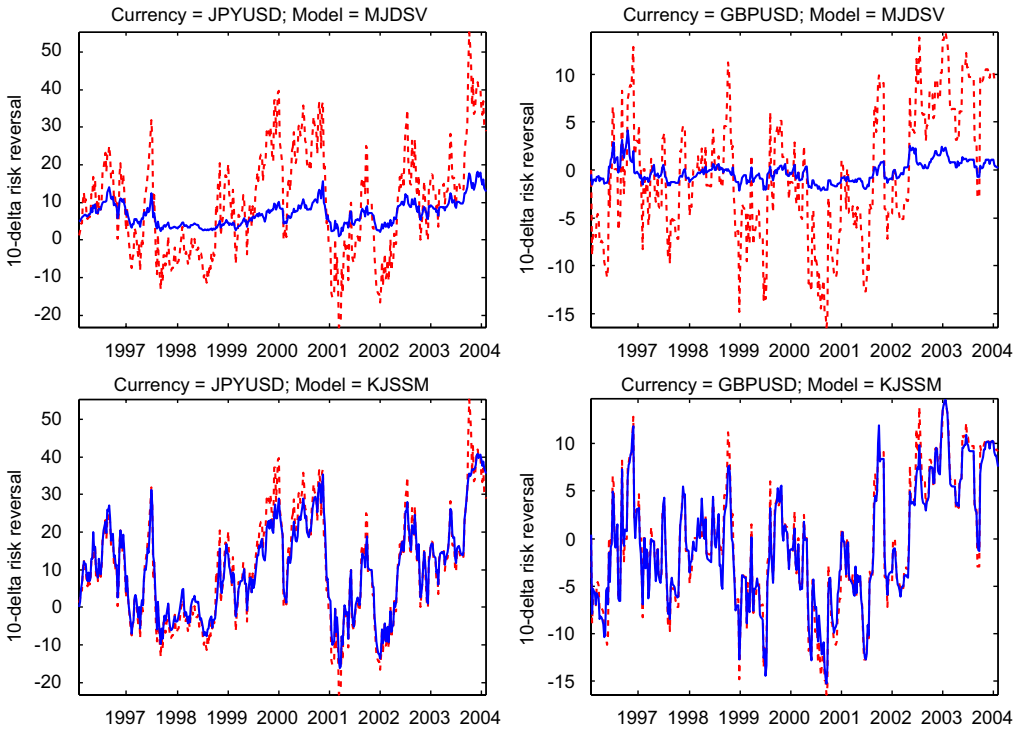

Fig. 7. Theory and evidence on the stochastic skew. Dashed lines are the market quotes on three-month ten-delta risk reversals, in percentages of the delta-neutral straddle implied volatility of the same maturity. Solid lines are the values computed from the estimated models using the whole sample of data.

5.5. *Theory and evidence on the stochastic skew*

The key feature that differentiates the implied volatility dynamics of currency options from their equity market counterparts is the strong time variation in the risk reversal, suggesting stochastic skewness in currency returns. Using the filtered time series on the activity rates, we compute the model implied option prices and implied volatilities. From the implied volatilities, we reconstruct the model implied risk reversals and compare them with the market observations.

Fig. 7 compares the time series of the observed risk reversals to the model implied values. For clarity, we plot only one time series for each currency pair: the ten-delta risk reversal at three-month maturity in percentages of the delta-neutral straddle implied volatility of the same maturity. The dashed lines denote data quotes, and the solid lines are the values computed from the estimated models.

The top two panels in Fig. 7 show that the MJDSV model fails miserably in capturing the observed strong variation in risk reversals. Compared with the strong variations in the data, the MJDSV model implied values vary very little. In contrast, the bottom two panels in Fig. 7 show that our SSM models can generate risk reversals variations that closely match those in the data. The matches are close to perfection except under extreme

realizations. Therefore, our SSM modeling framework contributes to the literature by capturing stochastic skew in addition to stochastic volatility, both of which are pervasive features of the currency options market.

6. Extensions

The class of stochastic skew models can in principle capture all of the salient features of currency option prices. The four SSM models that we have designed and estimated are extremely parsimonious as they have about the same number of free parameters as the Bates (1996b) model, and yet they generate much better performance by capturing an extra dimension of variation in the conditional skewness of the currency return distribution. In this section, we explore the virtues of more general specifications within the SSM model class.

6.1. Unconditional asymmetry

We achieve parsimony in the four estimated SSM models by assuming approximate unconditional symmetry on the currency return distribution. Based on this assumption, we use the same set of parameters to control the two Lévy components. The summary statistics in Table 1 suggests that the symmetry assumption holds reasonably well on GBPUSD, but less so on JPYUSD. For future applications, if we intend to price options on exchange rates between emerging markets and industrialized countries, this assumption is likely to be strongly violated because risk reversals on these currency pairs often skew toward the industrialized countries. For example, the option implied risk-neutral return distributions on the US dollar price of most emerging market currencies are negatively skewed (Carr and Wu, forthcoming).[2] Thus, to price options on these currency pairs, it is imperative to allow the parameters for the two Lévy components to be different.

To gauge the importance of the asymmetry generalization for option pricing on the two currency pairs under investigation, we estimate an asymmetric SSM specification that allows the parameters for the two Lévy components to be different. Given the observed relative insensitivity to the jump structure specification, we limit our estimation to one jump structure, the KJ specification with α fixed at -1. In this case, we have 15 model parameters: $\Theta \equiv [\sigma_r, (\sigma^2, \lambda, v_J, \kappa, \sigma_v, \kappa^P, \rho)_{R,L}]$, where the parameters with an R subscript are for the right skewed Lévy component and the parameters with an L subscript are for the left skewed Lévy component. We label this model as KJASSM, with the letter A denoting asymmetry. The option pricing formula can be derived analogously. We estimate the model using the first six years of data and compare its performance with its symmetric counterpart KJSSM both in sample and out of sample.

Table 8 reports the estimation results. In the top panel, we report the parameters and their standard errors (in parentheses) that govern the two Lévy components. We also report their differences and the absolute magnitudes of the t-statistics on the differences. The average magnitudes of the two Lévy components are controlled by $\sigma^2_{R,L}$ for the two diffusion components and $\lambda_{R,L}$ for the two jump components. For JPYUSD, the estimates are markedly different for the right and left skewed Lévy components. The average

[2]Another example is equity index options. The slopes of the implied volatility smiles are time varying, but they stay negative most of the time.

Table 8
Likelihood estimation of the asymmetric model KJASSM

Entries report the maximum likelihood estimates of the model parameters and their standard errors (in parentheses) for KJASSM. We also report the difference between the parameters for the right skewed Lévy component and the corresponding parameters for the left skewed Lévy component, as well as the absolute magnitude of the t-statistics on the difference. For model performance, we report the root mean squared pricing error (rmse) in implied volatility percentage points, the mean weekly log likelihood ($\mathscr{L}/N$), and the likelihood ratio statistic against the KJSSM model, $LR = 2(\mathscr{L}_{KJASSM} - \mathscr{L}_{KJSSM})$, which has a chi-square distribution with six degrees of freedom. The critical value for the statistic at 99% confidence level is 16.81. The estimation uses the first six years of weekly option data from January 24, 1996 to December 26, 2001 (310 weekly observations for each series). In-sample performance measures are based on the same sample period. Out-of-sample performance measures are based on the remaining two years of data from January 2, 2002 to January 28, 2004 (109 weekly observations for each series).

Currency	JPYUSD						GBPUSD					
Θ	Right		Left		Difference	$\lvert t\rvert$-value	Right		Left		Difference	$\lvert t\rvert$-value
σ^2	1.004	(4.249)	0.007	(0.004)	0.998	0.235	0.005	(0.004)	0.023	(0.016)	−0.018	1.375
λ	8.065	(34.299)	0.005	(10.113)	8.060	0.219	0.078	(4.200)	0.063	(0.043)	0.016	0.004
v_j	0.030	(0.001)	0.000	(0.177)	0.030	0.167	0.001	(0.024)	0.061	(0.003)	−0.060	2.402
κ	0.003	(0.012)	20.037	(0.232)	−20.034	87.665	5.636	(0.039)	0.014	(0.011)	5.622	133.24
σ_v	0.212	(0.450)	11.665	(0.159)	−11.452	26.972	5.781	(0.066)	0.126	(0.043)	5.656	72.082
ρ	0.000	(0.003)	−0.042	(0.008)	0.042	4.408	0.179	(0.068)	−0.998	(0.036)	1.179	0.004
κ^P	0.906	(0.443)	2.467	(0.576)	−1.561	1.924	2.240	(0.493)	0.077	(0.008)	2.163	4.392
In-sample performance:												
rmse				0.65						0.33		
$\mathscr{L}/N$				−6.50						23.15		
LR				6265.60						6746.47		
Out-of-sample performance:												
rmse				0.75						0.26		
$\mathscr{L}/N$				−13.24						28.96		
LR				1139.66						1234.18		

magnitudes of the right skewed component are much larger than the average magnitudes of the left skewed component, generating positive risk reversals and positively skewed conditional currency return distribution on average. Nevertheless, the estimates also show large standard errors, making the differences statistically insignificant.

For GBPUSD, the (σ^2, λ) estimates for the two Lévy components show smaller differences, consistent with the smaller average risk reversals. Again, the standard errors of the estimates are large and the parameter differences between the two components are insignificant. The large standard errors for both currency pairs suggest that the fully asymmetric specification experiences some identification issues.

The t-statistics on the parameter differences show that the most significant asymmetry between the two Lévy components do not come from their average magnitudes (σ^2, λ), but from the risk-neutral persistence (κ) and, to a lesser degree, volatility (σ_v) of the two underlying activity rates. For JPYUSD, the activity rate for the right skewed Lévy component is more persistent but less volatile than the activity rate for the left skewed Lévy component. The opposite is the case for GBPUSD.

Table 8 also reports the in-sample and out-of-sample performance for the asymmetric model. The in-sample root mean squared pricing errors are 0.65 for JPYUSD and 0.33 for GBPUSD, substantially smaller than the corresponding values (0.89 and 0.42) for its symmetric counterpart (KJSSM in Table 6). We also report the likelihood ratio test statistics between the two models, $LR = 2(\mathscr{L}_{KJASSM} - \mathscr{L}_{KJSSM})$, which has a chi-square distribution with six degrees of freedom. The critical value at the 99% confidence level is 16.81. The LR statistics show that KJASSM significantly outperforms its symmetric counterpart KJSSM.

6.2. Stochastic central tendency

The mean absolute pricing errors in Fig. 5 show that the KJSSM model performs better on three-month options than on one- and 12-month options, pointing to remaining tensions along the term structure dimension. Furthermore, the summary statistics in Table 1 show that the weekly autocorrelation estimates for risk reversals, butterfly spreads, and delta-neutral straddle implied volatilities all increase with option maturities. The upward sloping term structure on the autocorrelation estimates suggests the potential existence of multiple volatility factors with different persistence, with low persistence factors dominating short term contracts and high persistence factors dominating long term contracts. Finally, when we allow the two Lévy components in the SSM model to be asymmetric in KJASSM, the most significant asymmetry identified from the estimation does not come from the average magnitudes of the two Lévy components, but from the persistence of the two underlying activity rates.

Based on these observations, we consider an alternative generalization of the KJSSM model by allowing the mean of the two activity rates to be stochastic and driven by one common dynamic factor:

$$\begin{aligned} \mathrm{d}v_t^j &= \kappa(\theta_t - v_t^j)\,\mathrm{d}t + \sigma_v\sqrt{v_t^j}\,\mathrm{d}Z_t^j, \quad j = R, L, \\ \mathrm{d}\theta_t &= \kappa_\theta(1-\theta_t)\,\mathrm{d}t + \sigma_\theta\sqrt{\theta_t}\,\mathrm{d}Z_t^\theta, \end{aligned} \tag{29}$$

where θ_t denotes the common stochastic central tendency (Balduzzi, Das, and Foresi, 1998) for the two activity rates and Z_t^θ denotes another standard Brownian motion that is

independent of other Brownian motions. We label this extended model as KJSSMSC, with SC denoting the stochastic central tendency generalization. In contrast to KJASSM, KJSSMSC retains the symmetric assumption but allows the activity rate dynamics for each Lévy component to be controlled by two factors with different persistence. Normally, the stochastic central tendency factor is more persistent than the activity rate itself: $\kappa_\theta < \kappa$. Long term option contracts depend more heavily on the central tendency factor and hence show higher persistence.

Under this specification, we can show that the generalized Fourier transform of the currency return remains exponential affine in the current levels of the expanded state vector $V_0 \equiv [v_0^R, v_0^L, \theta_0]$,

$$\phi_s(u) = \exp(iu(r_d - r_f)t - b(t)^\top V_0 - c(t)), \tag{30}$$

where the coefficients $[b(t), c(t)]$ solve a set of ordinary differential equations:

$$b'(t) = b_v - K^\top b(t) - \tfrac{1}{2}\Sigma \odot b(t) \odot b(t), \quad c'(t) = b(t)^\top M, \tag{31}$$

Table 9
Likelihood estimation of the stochastic central tendency model KJSSMSC

Entries report the maximum likelihood estimates of the model parameters and their standard errors (in parentheses) for KJSSMSC. For model performance, we report the root mean squared pricing error (rmse) in implied volatility percentage points, the mean weekly log likelihood ($\mathscr{L}/N$), and the likelihood ratio statistic against the KJSSM model, $LR = 2(\mathscr{L}_{KJSSMSC} - \mathscr{L}_{KJSSM})$, which has a chi-square distribution with 313 degrees of freedom for in-sample performance and 112 degrees of freedom for out-of-sample performance. The critical value of the statistic at 99% confidence level is 374.13 (in-sample) and 149.73 (out-of-sample), respectively. The estimation uses the first six years of weekly option data from January 24, 1996 to December 26, 2001 (310 weekly observations for each series). In-sample performance measures are based on the same sample period. Out-of-sample performance measures are based on the remaining two years of data from January 2, 2002 to January 28, 2004 (109 weekly observations for each series).

Currency	JPYUSD		GBPUSD	
σ^2	0.033	(0.012)	0.002	(0.000)
λ	0.098	(0.038)	1.104	(0.146)
v_j	0.092	(0.001)	0.002	(0.000)
κ	23.028	(0.144)	8.184	(0.027)
σ_v	1.764	(0.343)	3.980	(0.046)
ρ^R	0.587	(0.020)	0.703	(0.052)
ρ^L	−0.730	(0.026)	−0.993	(0.073)
κ^P	1.180	(0.114)	3.192	(0.319)
κ_θ	0.027	(0.011)	0.193	(0.006)
σ_θ	0.224	(0.042)	0.617	(0.010)
κ_θ^P	0.171	(0.177)	0.194	(0.010)
σ_r	0.251	(0.001)	0.039	(0.000)
In-sample performance:				
rmse	0.49		0.22	
$\mathscr{L}/N$	2.74		37.61	
LR	11998.70		15711.15	
Out-of-sample performance:				
rmse	0.52		0.20	
$\mathscr{L}/N$	2.81		39.79	
LR	4638.85		3594.54	

with $\odot$ denoting the Hadamard product and

$$b_v = \begin{bmatrix} \psi^R \\ \psi^L \\ 0 \end{bmatrix}, \quad K = \begin{bmatrix} \kappa - \mathrm{i}u\sigma\sigma_v\rho^R & 0 & -\kappa \\ 0 & \kappa - \mathrm{i}u\sigma\sigma_v\rho^L & -\kappa \\ 0 & 0 & \kappa_\theta \end{bmatrix}, \quad \Sigma = \begin{bmatrix} \sigma_v^2 \\ \sigma_v^2 \\ \sigma_\theta^2 \end{bmatrix},$$
$$M = \begin{bmatrix} 0 \\ 0 \\ \kappa_\theta \end{bmatrix}. \tag{32}$$

The coefficients can be solved numerically starting at $b(0) = 0$ and $c(0) = 0$.

We estimate this stochastic central tendency model using the first six years of data and compare its performance with KJSSM both in sample and out of sample. We assume that the market price of θ_t risk is proportional to $\sqrt{\theta_t}$ and use κ_θ^P to denote the mean reversion coefficient for θ_t under the statistical measure $\mathbb{P}$. Compared with KJSSM, this new model KJSSMSC has three additional parameters $(\kappa_\theta, \sigma_\theta, \kappa_\theta^P)$ that control the risk-neutral and statistical dynamics of the stochastic central tendency factor θ_t.

Table 9 reports the parameter estimates and standard errors in the first panel, the in-sample performance measures in the second panel, and the out-of-sample performance measures in the third panel. The parameter estimates show that the central tendency factor θ_t is much more persistent than the activity rates themselves under both the risk-neutral measure and the statistical measure. The performance measures show that the addition of the central tendency factor dramatically improves the model performance. The root mean squared errors are much smaller and the likelihood values are much larger than both the KJSSM benchmark and the asymmetric generalization KJASSM. The root mean squared errors for KJSSMSC are only about half of that for KJSSM. The likelihood ratio test statistics, $LR = 2(\mathscr{L}_{KJSSMSC} - \mathscr{L}_{KJSSM})$, are very large and highly significant over any reasonable confidence level both in sample and out of sample.

7. Conclusions

In this paper, we analyze the statistical properties of currency option implied volatilities across the dimensions of moneyness, maturity, and calendar time. We find that the market prices of currency options exhibit several behaviors that challenge standard models in the option pricing literature. Chief among these challenging behaviors is the observation that the risk reversals vary greatly over time and switch signs several times in our sample.

Working within the paradigm of time-changed Lévy processes, we develop and estimate a subclass of models that captures this stochastic skew behavior of currency option prices. Our estimation results show that our stochastic skew models strongly outperform traditional jump-diffusion stochastic volatility models, both in sample and out of sample.

For future research, it is important to understand the economic underpinnings of the stochastic skewness suggested by currency option prices. An understanding of the source of this feature should have important implications on our understanding of the behavior of currency risk premia. For such research, our stochastic skew modeling framework can serve as a benchmark, upon which we can construct the pricing kernels for each economy

and link the exchange rate dynamics to the ratio of the pricing kernels of the two relevant economies.

References

Andrews, D., 1991. Heteroskedasticity and autocorrelation consistent covariance matrix estimation. Econometrica 59, 817–858.

Bakshi, G., Chen, Z., 1997. Equilibrium valuation of foreign exchange claims. Journal of Finance 52, 799–826.

Balduzzi, P., Das, S., Foresi, S., 1998. The central tendency: a second factor in bond yields. Review of Economics and Statistics 80, 62–72.

Bates, D., 1996a. Dollar jump fears 1984–1992: distributional abnormalities implicit in foreign currency futures options. Journal of International Money and Finance 15, 65–93.

Bates, D., 1996b. Jumps and stochastic volatility: exchange rate processes implicit in deutsche mark options. Review of Financial Studies 9, 69–107.

Bertoin, J., 1996. Lévy Processes. Cambridge University Press, Cambridge, UK.

Bollen, N.P., 1998. Valuing options in regime-switch models. Journal of Derivatives 6, 38–49.

Bollen, N.P., Raisel, E., 2003. The performance of alternative valuation models in the OTC currency option market. Journal of International Money and Finance 22, 33–64.

Bollen, N.P., Gray, S.F., Whaley, R.E., 2000. Regime-switching in foreign exchange rates: evidence from currency option prices. Journal of Econometrics 94, 239–276.

Campa, J.M., Chang, P.H.K., 1995. Testing the expectations hypothesis on the term structure of volatilities in foreign exchange options. Journal of Finance 50, 529–547.

Campa, J.M., Chang, P.H.K., 1998. The forecasting ability of correlations implied in foreign exchange options. Journal of International Money and Finance 17, 855–880.

Campa, J.M., Chang, P.H.K., Reider, R.L., 1998. Implied exchange rate distributions: evidence from OTC options market. Journal of International Money and Finance 17, 117–160.

Carr, P., Wu, L., 2003. Finite moment log stable process and option pricing. Journal of Finance 58, 753–777.

Carr, P., Wu, L., 2004. Time-changed Lévy processes and option pricing. Journal of Financial Economics 71, 113–141.

Carr, P., Wu, L., forthcoming. Theory and evidence on the dynamics interactions between sovereign credit default swaps and currency options. Journal of Banking and Finance.

Carr, P., Geman, H., Madan, D., Yor, M., 2002. The fine structure of asset returns: an empirical investigation. Journal of Business 75, 305–332.

Daal, E., Madan, D., 2005. An empirical investigation of the variance-gamma model for foreign currency options. Journal of Business 78, 2121–2152.

Foresi, S., Wu, L., 2005. Crash-o-phobia: a domestic fear or a worldwide concern? Journal of Derivatives 13, 8–21.

Garman, M., Kohlhagen, S., 1983. Foreign currency option values. Journal of International Money and Finance 2, 231–237.

Heston, S., 1993. Closed-form solution for options with stochastic volatility, with application to bond and currency options. Review of Financial Studies 6, 327–343.

Huang, J., Wu, L., 2004. Specification analysis of option pricing models based on time-changed Lévy processes. Journal of Finance 59, 1405–1440.

Hull, J., White, A., 1987. The pricing of options on assets with stochastic volatilities. Journal of Finance 42, 281–300.

Johnson, T.C., 2002. Volatility, momentum, and time-varying skewness in foreign exchange returns. Journal of Business and Economic Statistics 20, 390–411.

Kalman, R.E., 1960. A new approach to linear filtering and prediction problems. Transactions of the ASME—Journal of Basic Engineering 82, 35–45.

Kou, S.G., 2002. A jump-diffusion model for option pricing. Management Science 48, 1086–1101.

Madan, D., Seneta, E., 1990. The variance gamma (V.G.) model for share market returns. Journal of Business 63, 511–524.

Madan, D.B., Carr, P.P., Chang, E.C., 1998. The variance gamma process and option pricing. European Finance Review 2, 79–105.

Merton, R.C., 1976. Option pricing when underlying stock returns are discontinuous. Journal of Financial Economics 3, 125–144.

Newey, W.K., West, K.D., 1987. A simple, positive semi-definite, heteroskedasticity and autocorrelation consistent covariance matrix. Econometrica 55, 703–708.

Vuong, Q.H., 1989. Likelihood ratio tests for model selection and non-nested hypotheses. Econometrica 57, 307–333.

Wan, E.A., van der Merwe, R., 2001. The unscented Kalman filter. In: Haykin, S. (Ed.), Kalman Filtering and Neural Networks. Wiley, New York.

Wu, L., 2006. Dampened power law: reconciling the tail behavior of financial asset returns. Journal of Business 79, 1445–1474.